Article

The PPH1 phosphatase is specifically involved in LHCII dephosphorylation and state transitions in Arabidopsis

SHAPIGUZOV, Alexey, *et al*.

Abstract

The ability of plants to adapt to changing light conditions depends on a protein kinase network in the chloroplast that leads to the reversible phosphorylation of key proteins in the photosynthetic membrane. Phosphorylation regulates, in a process called state transition, a profound reorganization of the electron transfer chain and remodeling of the thylakoid membranes. Phosphorylation governs the association of the mobile part of the light-harvesting antenna LHCII with either photosystem I or photosystem II. Recent work has identified the redox-regulated protein kinase STN7 as a major actor in state transitions, but the nature of the corresponding phosphatases remained unknown. Here we identify a phosphatase of Arabidopsis thaliana, called PPH1, which is specifically required for the dephosphorylation of light-harvesting complex II (LHCII). We show that this single phosphatase is largely responsible for the dephosphorylation of Lhcb1 and Lhcb2 but not of the photosystem II core proteins. PPH1, which belongs to the family of monomeric PP2C type phosphatases, is a chloroplast protein and is mainly associated with the [...]

Reference

SHAPIGUZOV, Alexey, *et al*. The PPH1 phosphatase is specifically involved in LHCII dephosphorylation and state transitions in Arabidopsis. *Proceedings of the National Academy of Sciences of the United States of America*, 2010, vol. 107, no. 10, p. 4782-7

DOI : 10.1073/pnas.0913810107
PMID : 20176943

The PPH1 phosphatase is specifically involved in LHCII dephosphorylation and state transitions in Arabidopsis

Alexey Shapiguzov [+,1,4], Björn Ingelsson [+,2], Iga Samol[1], Charles Andres[3], Felix Kessler[3], Jean-David Rochaix[1], Alexander V. Vener[2] and Michel Goldschmidt-Clermont[1]

+: These authors contributed equally to this work.

1: Departments of Plant Biology and of Molecular Biology, University of Geneva, Quai E. Ansermet 30, 1211 Genève 4, Switzerland
2: Department of Clinical and Experimental Medicine, Linköping University, SE-581 85 Linköping, Sweden
3: University of Neuchâtel, Institute of Biology, Rue Emile Argand 11, CP 158, 2009 Neuchâtel, Switzerland
4: Permanent address: Institute of Plant Physiology, Russian Academy of Sciences, Botanicheskaya 35, 127276 Moscow, Russia.

ABSTRACT

The ability of plants to adapt to changing light conditions depends on a protein kinase network in the chloroplast which leads to the reversible phosphorylation of key proteins in the photosynthetic membrane. Phosphorylation regulates, in a process called state transition, a profound reorganization of the electron transfer chain and remodeling of the thylakoid membranes. Phosphorylation governs the association of the mobile part of the light-harvesting antenna LHCII with either photosystem I or photosystem II. Recent work has identified the redox-regulated protein kinase STN7 as a major actor in state transitions, but the nature of the corresponding phosphatases remained unknown. Here we identify a single phosphatase of *Arabidopsis thaliana*, called PPH1, which is specifically required for the dephosphorylation of light-harvesting complex II (LHCII). We show that this single phosphatase is largely responsible for the dephosphorylation of Lhcb1 and Lhcb2, but not of the photosystem II core proteins. PPH1, which belongs to the family of monomeric PP2C type phosphatases, is a chloroplast protein and is mainly associated with the stroma lamellae of the thylakoid membranes. We demonstrate that loss of PPH1 leads to an increase in the antenna size of photosystem I and to a strong impairment of state transitions. Thus phosphorylation and dephosphorylation of LHCII appear to be specifically mediated by the kinase / phosphatase pair, STN7 and PPH1. These two proteins emerge as key players in the adaptation of the photosynthetic apparatus to changes in light quality and quantity.

\body

INTRODUCTION

Plants are critically dependent on light as a source of energy to drive photosynthesis. However in natural settings, both the intensity and the spectral quality of light vary extensively, sometimes within very short periods. Photosynthetic organisms posess an arsenal of mechanisms to adapt to such changes in their light environment, to optimize photosynthesis, prevent photo-oxidation in excess light and repair photo-damage (1, 2). These mechanisms operate on different time scales ranging from seconds to days, and at all levels of organization, from the photosynthetic complexes in the thylakoid membranes to the morphology of the whole plant. Under low light intensity, light harvesting is maximized, but under excess light, acclimation responses lead to reduced light capture and enhanced energy dissipation.

Two photosystems (PSII and PSI) together with their associated light-harvesting antennae function in series to drive linear electron flow in the thylakoid membranes, leading to the production of ATP and reductants such as reduced ferredoxin or NADPH. Cyclic electron flow around PSI allows for the synthesis of ATP without generating reducing power. Thus, the balance between linear and cyclic electron flow influences the ATP energy charge as well as the redox poise of the plant cell (2). The two photosystems have different light-absorption characteristics, and depending on the spectral composition of ambient light, a process called state transition regulates the relative cross-sections of their antennae to optimize linear electron flow (3-5). In the green alga Chlamydomonas, state transitions also modulate cyclic electron flow and play a major regulatory role to respond to the metabolic requirements for ATP (6).

Two prominent features of state transitions are (i) the association of a mobile part of the LHCII antenna with either PSII or PSI, and (ii) changes in the structural organization of the thylakoid membranes. In state 1, the antenna is attached to PSII in grana stacks of the thylakoid membranes. In state 2 part of the antenna migrates and associates with PSI in stroma lamellae, grana margins and grana ends, with a concomitant destacking of the thylakoid membranes (7, 8). State transitions are regulated by a protein kinase, called STN7 in Arabidopsis or Stt7 in Chlamydomonas, which is involved in the phosphorylation of some of the LHCII proteins (9-11). The activity of the kinase is controlled by the redox state of the plastoquinone pool, or more specifically by binding of reduced plastoquinol to the Q_o site of the b_6f complex (12, 13). Thus, when light conditions favor the activity of PSII, reduction of the plastoquinone pool activates the STN7 kinase and causes a transition to state 2. The LHCII antenna is phosphorylated (5) and associates with PSI by binding to the PsaH subunit (14). The process is reversible, so that when PSI is more active and the plastoquinone pool is oxidized, the LHCII antenna is dephosphorylated and associates with PSII. While the corresponding phosphatase activity has been assayed in thylakoid preparations, little is known on the molecular nature of the phosphatases involved in state transitions (15). Dephosphorylation of LHCII proteins was observed with isolated thylakoids indicating that at least a portion of the phosphatase is membrane-associated (16). It was further shown that thylakoid protein phosphatases are redox-independent and kinetically heterogeneous (17). A 29 kDa stromal protein phosphatase was shown to act on LHCII *in vitro* (18). However it is not clear whether this protein functions in the dephosphorylation of LHCII *in vivo.* Here we report the identification of a chloroplast protein phosphatase, PPH1, which is specifically

required for efficient dephosphorylation of the LHCII antenna and transition from state 2 to state 1.

RESULTS

A genetic screen for phosphatases involved in state transitions

Comprehensive genomic surveys identified 159 genes that code for catalytic subunits of protein phosphatases in Arabidopsis (19-21). We included all of these proteins, as well as others that are annotated in the Interpro database to contain domains of phosphatase regulatory subunits, in an initial candidate list. Their subcellular localization was predicted *in silico* using a panel of eight algorithms available through the Suba II website (22). Those phosphatases that were predicted by at least one program to be targeted to the plastid were retained, and ordered according to the number of different algorithms that predicted plastid localization. Data from mass spectrometric analysis of chloroplast proteins was also taken into account (23, 24). Co-expression of the putative chloroplast phosphatase genes with *STN7* and *STN8*, based on an analysis of publicly available micro-array data using the Genevestigator clustering tool (25) was used as a further criterion to rank the candidates. We obtained 84 homozygous T-DNA insertion lines disrupting the genes encoding 60 putative chloroplast phosphatases, and systematically analyzed seedlings for defects in protein dephosphorylation during a transition from state 2 to state 1, using the immunoblotting assay described in the next section. One of the high-ranking candidates, *pph1-1*, showed a strong defect in dephosphorylation of the LHCII antenna, and was selected for further analysis.

The PPH1 phosphatase is required for the dephosphorylation of the LHCII antenna

When Arabidopsis seedlings are exposed to moderate levels of white light (50 $\mu E\ m^{-2}\ s^{-1}$), their photosynthetic electron transfer chain is largely in state 2. Reduction of the plastoquinone pool leads to the association of the mobile part of the LHCII antenna with PSI and to the phosphorylation of the Lhcb proteins which can be monitored by immunoblotting with anti-phosphothreonine antibodies (Fig 1A) (26). Other proteins of the thylakoid membrane are also phosphorylated, such as CP43, D1 and D2 which are subunits of the PSII core (27). Upon exposure to far-red light, excitation of PSI is favored over PSII, so that the plastoquinone pool is oxidized and the system shifts to state 1. The mobile LHCII antenna associates with PSII and the LHCII proteins are dephosphorylated (Fig 1A). There is also a decrease in the phosphorylation of D1 and D2, and to a lesser degree of CP43. Phosphorylation of LHCII is strongly reduced after 20 minutes of exposure to far-red light and reaches a low level after 40 minutes in our experimental conditions. A similar effect is observed when seedlings are transferred from white light to the dark. Phosphorylation is rapidly restored if the seedlings are transferred from far-red light to blue light which induces a transition to state 2.

In striking contrast, in *pph1* mutants LHCII remained strongly phosphorylated after 20 minutes of far-red light treatment and showed only a moderate decrease after 40 minutes (Fig 1B). The effect appears to be specific for LHCII because the core subunits of PSII underwent dephosphorylation as in the wild type. Impaired dephosphorylation of LHCII proteins was similarly observed in *pph1* mutants when a transition from state 2 to state 1 was induced by transferring adult plants from moderate white light to the dark (Fig. 1C). These observations identified the PPH1 phosphatase as an essential component required

for the dephosphorylation of the LHCII antenna, but not of the PSII core, during a transition from state 2 to state 1. Although in *pph1* mutants dephosphorylation was impaired during a transition to state 1, there was no apparent hyper-phosphorylation of the Lhcb proteins under the conditions favoring state 2 which were used for growing the seedlings (moderate white light, 50 μE m^{-2} s^{-1}).

Analysis of *in vivo* protein phosphorylation in *pph1-1* by mass spectrometry

Immunoblotting analysis of Arabidopsis seedlings exposed to far-red light showed that phosphorylation of LHCII proteins was significantly reduced in the wild-type but not in *pph1-1* plants (Fig. 1B). The LHCII antenna comprises many isoforms of the Lhcb proteins. To determine more precisely which Lhcb polypeptides were not dephosphorylated in the mutant, we analyzed these proteins using differential stable isotope labeling and mass spectrometry (see Supporting Information). After exposure to far-red light, thylakoid membranes were isolated in parallel from the *pph1-1* mutant and wild-type plants in the presence of NaF to inhibit dephosphorylation (28). The surface-exposed peptides from the wild-type and the mutant membranes were prepared by proteolytic shaving and were differentially labeled by esterification of carboxylic groups with hydrogen- or deuterium-containing methanol respectively (29, 30). A 1:1 mixture of these two preparations was subjected to IMAC (immobilized metal ion affinity chromatography) so as to capture and enrich the phosphorylated peptide methyl esters. The phosphorylated peptides enriched by IMAC were then subjected to nano liquid chromatography and electrospray ionization mass spectrometry (LC-MS) which allowed for simultaneous measurements of light- and heavy-isotope labeled phosphopeptide pairs. We also performed the reverse labeling of the wild-type and mutant peptides as an internal control and additional experiment for relative quantification of differentially labeled peptides. The difference in intensities of "light" and "heavy" phosphorylated peptides provided quantitative data for the phosphorylation differences between the mutant and wild-type after a transition from state 2 to state 1 induced with far-red light. (Figs. S1-S3).

The LC-MS analyses (Table 1; Figs. S1-S3) revealed very similar levels of phosphorylation for the photosystem II core proteins D1 and D2, but marked differences for the Lhcb proteins in the mutant compared to the wild type. In our analyses we found two phosphorylated peptides from LHCII proteins. However, it should be noted that because the Lhcb isoforms have very similar sequences, a specific peptide sequence can originate from several gene products. Importantly, we found that each of these two phosphopeptides was present in significantly higher amounts in the mutant samples than in the wild type (Table 1). Thus, our data reveal that PPH1 deficiency resulted in significantly higher phosphorylation of LHCII peptides which could correspond to up to seven different Lhcb gene products.

Alternative splicing of *PPH1* mRNA

Three alternative transcript models are annotated for the PPH1 gene on the Arabidopsis Information Resource (TAIR) website (31). The longest open reading frame corresponds to a fully spliced mRNA that contains 11 exons and is predicted to encode a 43 kDa polypeptide (Fig S4, AT4G27800.1). Reverse transcription followed by PCR and sequencing confirmed the presence of this mature mRNA in rosette leaves (Fig. S5A). A

longer alternatively spliced form of the mRNA was also observed (AT4G27800.2), which retains intron 9 and is predicted to encode a truncated 36 kDa polypeptide that lacks some of the highly conserved residues of PP2C phosphatases (Fig. S4). The longer predicted isoform of PPH1 has a single potential hydrophobic transmembrane helix, while the shorter predicted isoform may be a soluble protein (Fig. S4). We could not confirm the presence of a third form of the transcript, which would have contained a four base-pair insert at the end of exon 8. We obtained three alleles with T-DNA insertions in the *PPH1* gene (Fig. S4). Two alleles, *pph1-1* and *pph1-2*, have insertions in the 5'UTR of the gene. Another allele, *pph1-3*, has an insertion in exon 4.
In order to assess whether the mutations are null or hypomorphic, we examined the level of expression of the *PPH1* gene. RNA was extracted from leaves of wild-type and *pph1* mutant plants and analyzed by RNA-blotting with a *PPH1* probe. The *pph1-2* and *pph1-3* plants had no detectable *PPH1* mRNA. However the *pph1-1* mutant showed residual levels of *PPH1* mRNA, which accumulated to approximately a third of the amount in the wild-type (Fig. S5B). These data indicate that the *pph1-1* mutant is leaky and that residual levels of the phosphatase may be present in the *pph1-1* plants. This suggests that only partial defects should be expected in the phenotypic analysis of the *pph1-1* mutant plants.

The PPH1 phosphatase is a chloroplast protein
To determine whether PPH1 is targeted to the chloroplast, ^{35}S-labeled PPH1 preprotein was obtained by *in vitro* translation and presented to isolated chloroplasts in an *in vitro* import assay (Fig. 2A). After the incubation, the 44 kDa precursor was converted to a shorter form which was protected from exogenous protease, showing that pre-PPH1 is imported and processed in the chloroplast, to a mass corresponding to that of the predicted mature form. Moreover, the radio-labeled PPH1 precursor was also efficiently imported into isolated pea chloroplasts and processed to the mature form, which was protected from exogenous protease (Fig. 2B).
To investigate the subcellular localization of the protein *in vivo*, a PPH1::GFP gene fusion under the CaMV 35S promoter was used to transform *Nicotiana benthamia* leaf cells by agroinfiltration. Confocal microscopy confirmed that the PPH1::GFP fusion localizes to the chloroplast (Fig. 2C, 2D). The GFP signal formed distinct spots that suggested the fusion protein was localizing to a sub-compartment of the chloroplast. A similar pattern was previously observed with STN7::GFP (9).
To determine where PPH1 is localized inside chloroplasts, we generated an antibody against a specific peptide sequence in the central part of the mature protein. This antibody recognized a band migrating at approximately 40 kDa in immunoblots of wild-type chloroplast proteins (Fig. 3A). This corresponds to the size of the predicted mature form, and of the processed form observed in the *in vitro* import experiments. Comparison of chloroplasts from *pph1-1* mutant and wild-type plants demonstrated a significant reduction of the 40 kDa band, which can thus be identified as PPH1 (Fig 3A). These results are consistent with our finding that the *pph1-1* mutant showed reduced levels of *PPH1* mRNA (Fig. S5B). The nature of a cross-reacting band that migrated slightly faster is presently not known, but it was detected only when the proteins were separated in PAGE gels containing urea (Fig. 3A), but not in those without urea (Fig. 3B). Immunoblots of membrane / thylakoid and soluble chloroplast fractions showed that a

large portion of the PPH1 protein was present in the thylakoid membranes. Although it was also detected in the soluble fraction, its relative amount compared to the large subunit of Rubisco was much lower than in the total chloroplast sample, indicating that PPH1 is not enriched in the stroma. Further fractionation of thylakoid membrane domains by centrifugation after treatment with digitonin revealed that the phosphatase was highly enriched in stroma lamellae, while its signal in the grana fraction was significantly lower (Fig. 3B). These data indicate that in chloroplasts a large portion of PPH1 resides at the stroma lamellae of thylakoid membranes.

The PPH1 phosphatase is involved in state transitions

In state transitions, association of part of LHCII with either PSII or PSI causes changes in the relative cross-sections of their respective antennae. This can be monitored by determining the low temperature fluorescence emission spectra of crude thylakoid preparations (Fig. 4A). For this analysis, leaves in state 1 and state 2 were obtained by exposure to far-red and blue light, respectively. As a control, the *stn7* kinase mutant that is deficient in state transitions was also included in the analysis. A significant increase in PSI fluorescence was observed in wild-type seedlings in state 2 relative to state 1 (Fig. 4A). This difference was abolished in the *stn7* kinase mutant, which is locked in state 1 and did not show an increased PSI fluorescence under state 2 conditions. In *pph1-1*, the differences in PSI fluorescence levels observed between state 1 and state 2 conditions were significantly lower compared to the wild type, and in *pph1-2* and *pph1-3* they were reduced even more strongly. Under state 1 conditions, the *pph1* mutant seedlings showed higher relative PSI fluorescence than the wild type. This suggests that the defect in dephosphorylation caused a bias towards state 2, with a tendency for the mobile antenna to be retained at PSI.

State transitions can also be measured using pulse amplitude modulated (PAM) chlorophyll fluorescence spectroscopy at room temperature, to monitor changes in the light harvesting antenna associated with PSII. In this analysis, state transitions were strongly impaired in the *pph1-2* allele, and were also affected in *pph1-1* (Fig. 4B,C). The data also suggested that in the *pph1* mutants the plastoquinone pool tended to remain more oxidized than in the wild type, as might be expected if phosphatase deficiency favors the association of the mobile LHCII antenna with PSI.

DISCUSSION

Reversible phosphorylation is a widespread protein modification involved in the regulation of metabolism and in many signal transduction pathways. State transitions are a particularly striking example because the phosphorylation of thylakoid proteins causes a profound reorganization of the electron transfer chain and remodeling of the thylakoid membrane system. Together with the b_6f complex, the STN7 kinase acts as a sensor of the redox poise of the electron transfer chain, and relays this signal by phosphorylating numerous target proteins. This regulates both short term responses such as state transitions and long term responses involving changes in the composition of the photosynthetic machinery (32). To allow acclimation to fluctuating light conditions and homeostasis, such responses must be reversible and therefore require the activity of phosphatases. Here we identify the protein phosphatase, PPH1, which is largely responsible for the dephosphorylation of the LHCII antenna.

PPH1 belongs to the PP2C type of protein phosphatases. This family of monomeric enzymes has been widely expanded in plants, and includes 76 - 80 genes in Arabidopsis or 78 in rice, compared to only 18 in humans (20, 21). Phylogenetic comparisons show that PPH1 belongs to a distinct clade together with similar proteins from other plants, but does not have close paralogs in Arabidopsis (20, 33) (Fig. S6). Members of this clade share a characteristic additional domain (residues 242 – 274) featuring many basic amino acids which is absent in other PP2C phosphatases. Although it cannot be excluded that the role of PPH1 is indirect, the strong impairment of LHCII dephosphorylation in *pph1* mutants suggests that PPH1 is the major phosphatase for the LHCII proteins and that other phosphatases may play only a minor role. This lack of redundancy is consistent with the absence of close PPH1 paralogs in Arabidopsis, but is surprising because protein phosphatases are generally thought to be rather unspecific. In turn, PPH1 appears to be specific for the Lhcb polypeptides, since the dephosphorylation of the core proteins D1, D2 and CP43 of PSII is not affected in the mutants (Fig. 1). In state 2, phosphorylated LHCII is associated with PSI in the stroma-exposed parts of the thylakoid membrane network. Thus, the localization of PPH1 at the thylakoid membranes and particularly at stroma lamellae is consistent with the role of PPH1 in LHCII dephosphorylation and transition from state 2 to state 1.

Using reverse transcription and PCR, we have detected an alternatively spliced form of the *PPH1* mRNA in mature leaves. This form retains intron 9, which leads to a frame shift of the coding sequence and a premature stop codon. The predicted shorter truncated protein would lack residues that are highly conserved in PP2C phosphatases, as well as the putative hydrophobic transmembrane domain (Fig S4). It will be of interest to determine whether the alternative forms are differentially regulated and have different functions.

It has been clearly demonstrated that the STN7 kinase is required for the phosphorylation of LHCII and for transitions from state 1 to state 2. Because LHCII is the major target of STN7, this provides evidence that phosphorylation of the antenna plays a key role in state transitions. Consistent with this model, we have found that the PPH1 phosphatase, which is required for dephosphorylation of LHCII, is required for efficient transitions from state 2 to state 1. This was apparent both from chlorophyll fluorescence emission spectra at low temperature and from chlorophyll fluorescence analysis at room temperature (Fig. 4). Thus, the STN7 - PPH1 pair appears to be specific for the phosphorylation and dephosphorylation of the LHCII proteins respectively, and this correlates with their respective roles in state transitions.

After growth under conditions that favor state 2 (moderate white light), there is no apparent hyper-phosphorylation of LHCII in the *pph1* mutants. This is perhaps not surprising, since the activity of the LHCII kinase STN7 is known to be regulated by the redox state of the plastoquinone pool. In a *pph1* mutant, increased phosphorylation would result in enhanced association of the antenna with PSI. Increased PSI activity would in turn lead to oxidation of the plastoquinone pool, and therefore to reduced STN7 activity and diminished LHCII phosphorylation. Whether this negative feedback loop solely relies on the regulation of STN7 activity for homeostasis or whether the PPH1 phosphatase is also regulated remains to be determined.

In the *pph1-1* mutant, the levels of the *PPH1* mRNA are reduced approximately three-fold compared to the wild type. The drastic effect of this mutation on the

dephosphorylation of the LHCII antenna indicates that the reduced expression of *PPH1* mRNA strongly limits the levels of phosphatase activity in the mutant, and thus that there is probably no excess of the mRNA in the wild type. This may be important in appropriately balancing the level of activity of the phosphatase and of the STN7 kinase. This was also reflected in the analysis of state transitions where we found that the defect was more pronounced in the stronger alleles (*pph1-2* and *pph1-3*) than in the leaky allele (*pph1-1*). Consistently with this observation, dephosphorylation of LHCII in dark-adapted leaves was also more affected in a strong allele than in the weaker one (Fig. 1C). The phosphatase activities in isolated thylakoids were previously found to be kinetically heterogeneous, with LHCII being dephosphorylated fastest, followed by D1 and D2, and then CP43 and PsbH (17). The specificity of PPH1 for LHCII proteins that we have observed supports the hypothesis that several phosphatases must be involved in dephosphorylation of thylakoid phosphoproteins. Thus, the kinetic differences could either be due to the different properties of distinct enzymes, or to some different properties of the substrates. Although *in vitro* the phosphatase activities were reported not to be redox-regulated (17), evidence has also been presented that they could be modulated by light or reducing agents (34). Our identification of PPH1 will facilitate future studies on the role and the regulation of thylakoid protein phosphatases in light acclimation.

MATERIALS AND METHODS

Plant material and growth conditions

For the genetic screen *Arabidopsis thaliana* wild type plants and T-DNA insertion mutants (all of Columbia-0 ecotype) were grown on Murashige-Skoog agar supplemented with 1.5 % sucrose in a growth chamber (Percival CU36L5) in long days (16 h light / 8 h dark) at 22 °C under fluorescent white light (50 µE m^{-2} s^{-1}). Plants on soil were cultivated in growth chambers at 24 °C under white light (100 µE m^{-2} s^{-1}) in long days. Plants for chlorophyll fluorescence measurements were grown in short days (8 h light / 16 h dark). The T-DNA insertion lines (http://methylome.salk.edu/cgi-bin/homozygotes.cgi) (35) were obtained through the NASC (European Arabidopsis Stock Centre); *pph1-1*: SALK_025713C; *pph1-2*: SAIL_514-C03; *pph1-3*: GABI_232H12. The *stn7* mutant was described (9). Primers for genotyping are described in Supporting Information.

Bioinformatic tools

Searches for protein domains were performed on the InterPro web site (http://www.ebi.ac.uk/interpro/).
Subcellular localization was predicted with Suba II (http://www.plantenergy.uwa.edu.au/applications/suba/index.php).
Genomic data for Arabidopsis was obtained from TAIR (http://arabidopsis.org), and T-DNA insertion lines were searched on the Salk web site (http://methylome.salk.edu/cgi-bin/homozygotes.cgi).

Assays of thylakoid protein dephosphorylation

For far-red light treatment, 12-day old seedlings grown on agar plates were placed under panels of infrared LEDs (L735; Epitex, Kyoto, Japan). Liquid nitrogen frozen samples were ground 4 x 10 s in a triturator (Silamat S5; Ivoclar Vivadent AG, Schaan,

Liechtenstein) using pre-cooled glass beads. The frozen powder was thawed in 200 µL of lysis buffer containing 100 mM Tris-HCl, pH 7.7, 2 % SDS, 50 mM NaF, and 2 x Protease Inhibitor Cocktail (Sigma-Aldrich) and incubated for 30 min at 37 °C. The lysate was centrifuged for 10 min at 14 000 rpm at room temperature. The samples (0.3 µg Chl / lane) were separated by tris-glycine SDS-PAGE in 12 % acrylamide gels containing 6 M urea. Immunoblotting was performed using anti-phosphothreonine antibodies (Cell Signaling). The details of the quantitative mass-spectrometric analysis are provided in the Supporting Information.

In vitro import into isolated chloroplasts and localization of PPH1::GFP in tobacco
In vitro import into isolated chloroplasts was performed as described for pea and Arabidopsis (36, 37). Leaves of *Nicotiana benthamiana* were infiltrated with Agrobacterium *(35S::PPH1::GFP)* and after 48 h protoplasts were isolated and fluorescence was monitored using a laser scanning confocal microscope as described in Supporting Information.

Cell Fractionation
Chloroplasts and thylakoids were isolated essentially as in reference (38). The soluble stromal fraction was obtained as the supernatant after lysis of the chloroplasts. Fractionation of thylakoids into grana and stroma lamellae was performed by the use of digitonin. Thylakoids at a concentration of 0.6 mg of chlorophyll per mL were incubated with 1 % digitonin (Sigma-Aldrich) for five minutes and then centrifuged at 1 000 x g. The supernatant was collected and centrifuged at 40 000 x g for 40 min to pellet grana membranes and grana margins. The remaining supernatant was centrifuged at 140 000 x g to collect stroma lamellae.
Immunoblotting was performed essentially as described previously (39) by SDS-PAGE using 14 % acrylamide gels. Polyclonal antibody to PPH1 was raised against a synthetic peptide corresponding to residues 186 - 199 (Innovagen, Lund, Sweden). Antibodies towards D1, PsaF, Rubisco large subunit and Lhcb1 were purchased from Agrisera (Vännäs, Sweden).

Chlorophyll fluorescence measurements
Detached rosette leaves from short day-grown plants floating on distilled water in Petri dishes were placed under panels of far-red or blue LEDs (L735 and L470, Epitex, Kyoto, Japan) for 30 min to induce state 1 or state 2. Then leaves were frozen in liquid nitrogen and membrane extracts were prepared (see Supporting Information). Chlorophyll fluorescence at 77 K was recorded on a Jasco FP-750 spectrofluorometer. Excitation was at 480 nm (slit width 5 nm) and emission was recorded in the 600-800 nm range (slit width 5 nm). Room temperature chlorophyll fluorescence was recorded using an FMS1 Pulse Modulated Fluorimeter (Hansatech; Norfolk, England) as detailed in Supporting Information.

ACKNOWLEDGEMENTS
This work was supported by grants from SystemsX.ch (RTD project “Plant Growth in a Changing Environment”) to MGC and JDR as well as to FK, by grants from the Swedish Research Council, the Swedish Research Council for Environment, Agricultural Sciences

and Spatial Planning to AVV and from the NCCR Plant Survival and the Swiss National Foundation (3100AO-117712) to JDR and MGC. We thank Cyril Montandon and Birgit Agne for help with the *in vitro* import assays, Etienne Bucher for an actin probe and Nicolas Roggli for help with the figures.

References

1. Li Z, Wakao S, Fischer BB, & Niyogi KK (2009) Sensing and responding to excess light. *Annu Rev Plant Biol* 60:239-260.
2. Eberhard S, Finazzi G, & Wollman FA (2008) The dynamics of photosynthesis. *Annu Rev Genet* 42:463-515.
3. Wollman FA (2001) State transitions reveal the dynamics and flexibility of the photosynthetic apparatus. *EMBO J* 20:3623-3630.
4. Rochaix JD (2007) Role of thylakoid protein kinases in photosynthetic acclimation. *FEBS Lett* 581:2768-2775.
5. Allen JF (1992) Protein phosphorylation in regulation of photosynthesis. *Biochim Biophys Acta* 1098:275-335.
6. Finazzi G*, et al.* (2002) Involvement of state transitions in the switch between linear and cyclic electron flow in Chlamydomonas reinhardtii. *EMBO Rep* 3:280-285.
7. Tikkanen M*, et al.* (2008) Phosphorylation-dependent regulation of excitation energy distribution between the two photosystems in higher plants. *Biochim Biophys Acta* 1777:425-432.
8. Chuartzman SG*, et al.* (2008) Thylakoid membrane remodeling during state transitions in Arabidopsis. *Plant Cell* 20:1029-1039.
9. Bellafiore S, Barneche F, Peltier G, & Rochaix JD (2005) State transitions and light adaptation require chloroplast thylakoid protein kinase STN7. *Nature* 433:892-895.
10. Depege N, Bellafiore S, & Rochaix JD (2003) Role of chloroplast protein kinase Stt7 in LHCII phosphorylation and state transition in Chlamydomonas. *Science* 299:1572-1575.
11. Bonardi V*, et al.* (2005) Photosystem II core phosphorylation and photosynthetic acclimation require two different protein kinases. *Nature* 437:1179-1182.
12. Vener AV, van Kan PJ, Rich PR, Ohad I, & Andersson B (1997) Plastoquinol at the quinol oxidation site of reduced cytochrome bf mediates signal transduction between light and protein phosphorylation: thylakoid protein kinase deactivation by a single-turnover flash. *Proc Natl Acad Sci U S A* 94:1585-1590.
13. Zito F*, et al.* (1999) The Qo site of cytochrome b6f complexes controls the activation of the LHCII kinase. *EMBO J* 18:2961-2969.
14. Lunde C, Jensen PE, Haldrup A, Knoetzel J, & Scheller HV (2000) The PSI-H subunit of photosystem I is essential for state transitions in plant photosynthesis. *Nature* 408:613-615.
15. Aro EM & Ohad I (2003) Redox regulation of thylakoid protein phosphorylation. *Antioxid Redox Signal* 5:55-67.
16. Bennett J (1980) Chloroplast phosphoproteins. Evidence for a thylakoid-bound phosphoprotein phosphatase. *Eur J Biochem* 104:85-89.
17. Silverstein T, Cheng L, & Allen JF (1993) Chloroplast thylakoid protein phosphatase reactions are redox-independent and kinetically heterogeneous. *FEBS Lett* 334:101-105.
18. Hammer MF, Markwell J, & Sarath G (1997) Purification of a protein phosphatase from chloroplast stroma capable of dephosphorylating the light-harvesting complex-II. *Plant Physiol* 113:227-233.

19. Kerk D*, et al.* (2002) The complement of protein phosphatase catalytic subunits encoded in the genome of Arabidopsis. *Plant Physiol* 129:908-925.
20. Kerk D, Templeton G, & Moorhead GB (2008) Evolutionary radiation pattern of novel protein phosphatases revealed by analysis of protein data from the completely sequenced genomes of humans, green algae, and higher plants. *Plant Physiol* 146:351-367.
21. Xue T*, et al.* (2008) Genome-wide and expression analysis of protein phosphatase 2C in rice and Arabidopsis. *BMC Genomics* 9:550.
22. Heazlewood JL, Verboom RE, Tonti-Filippini J, Small I, & Millar AH (2007) SUBA: the Arabidopsis Subcellular Database. *Nucleic Acids Res* 35:D213-218.
23. van Wijk KJ (2004) Plastid proteomics. *Plant Physiol Biochem* 42:963-977.
24. Baerenfaller K*, et al.* (2008) Genome-scale proteomics reveals Arabidopsis thaliana gene models and proteome dynamics. *Science* 320:938-941.
25. Zimmermann P, Hennig L, & Gruissem W (2005) Gene-expression analysis and network discovery using Genevestigator. *Trends Plant Sci* 10:407-409.
26. Rintamaki E*, et al.* (1997) Phosphorylation of light-harvesting complex II and photosystem II core proteins shows different irradiance-dependent regulation in vivo. Application of phosphothreonine antibodies to analysis of thylakoid phosphoproteins. *J Biol Chem* 272:30476-30482.
27. Vener AV (2007) Environmentally modulated phosphorylation and dynamics of proteins in photosynthetic membranes. *Biochim Biophys Acta* 1767:449-457.
28. Vener AV, Rokka A, Fulgosi H, Andersson B, & Herrmann RG (1999) A cyclophilin-regulated PP2A-like protein phosphatase in thylakoid membranes of plant chloroplasts. *Biochemistry* 38:14955-14965.
29. Vener AV, Harms A, Sussman MR, & Vierstra RD (2001) Mass spectrometric resolution of reversible protein phosphorylation in photosynthetic membranes of Arabidopsis thaliana. *J Biol Chem* 276:6959-6966.
30. Ficarro SB*, et al.* (2002) Phosphoproteome analysis by mass spectrometry and its application to Saccharomyces cerevisiae. *Nat Biotechnol* 20:301-305.
31. Swarbreck D*, et al.* (2008) The Arabidopsis Information Resource (TAIR): gene structure and function annotation. *Nucleic Acids Res* 36:D1009-1014.
32. Pesaresi P*, et al.* (2009) Arabidopsis STN7 kinase provides a link between short- and long-term photosynthetic acclimation. *Plant Cell* 21:2402-2423.
33. Schweighofer A, Hirt H, & Meskiene I (2004) Plant PP2C phosphatases: emerging functions in stress signaling. *Trends Plant Sci* 9:236-243.
34. Hammer MF, Gautam S, Osterman JC, & Markwell J (1995) Assessing modulation of stromal and thylakoid light-harvesting complex-II phosphatase activities with phosphopeptide substrates. *Photosynthesis Reserarch* 44:107-115.
35. Alonso JM & Ecker JR (2006) Moving forward in reverse: genetic technologies to enable genome-wide phenomic screens in Arabidopsis. *Nat Rev Genet* 7:524-536.
36. Agne B*, et al.* (2009) A toc159 import receptor mutant, defective in hydrolysis of GTP, supports preprotein import into chloroplasts. *J Biol Chem* 284:8670-8679.
37. Smith MD, Fitzpatrick L, Keegstra K, & Schell DJ (2002) In Vitro Analysis of Chloroplast Protein Import. *Current Protocols in Cell Biology*), pp 11.16.11-11.16.21.

38. Schubert M*, et al.* (2002) Proteome map of the chloroplast lumen of Arabidopsis thaliana. *J Biol Chem* 277:8354-8365.
39. Ingelsson B, Shapiguzov A, Kieselbach T, & Vener AV (2009) Peptidyl-prolyl isomerase activity in chloroplast thylakoid lumen is a dispensable function of immunophilins in Arabidopsis thaliana. *Plant Cell Physiol* 50:1801-1814.

Figure Legends

Figure 1. Analysis of thylakoid protein dephosphorylation
(A) Dephosphorylation of thylakoid proteins. Twelve-day old Col0 wild-type seedlings grown under white light were exposed to far-red light or transferred to the dark for the indicated times to induce a transition from state 2 to state 1. Seedlings treated with far red for 1 hour were then exposed to blue light to induce the reverse transition from state 1 to state 2. Total protein was extracted, and analyzed by SDS-PAGE and immunoblotting with anti-phosphothreonine antibodies.
(B) The *pph1* mutants are deficient in LHCII dephosphorylation under far-red light. Seedlings of the Col0 wild-type (WT), of *pph1-1*, and of *pph1-2* were treated with far-red light and analyzed as in (A). The same blot was decorated with antibody against the PsaA subunit of PSI as a control.
(C) The *pph1* mutants are deficient in dark-induced LHCII dephosphorylation. Four hours after the onset of the light period, mature leaves were collected and the plants were transferred to the dark for 5 hours. Total protein was extracted and analyzed as in (A). Note that the defect in dephosphorylation is more pronounced in *pph1-3* than in *pph1-1*, which is a leaky allele containing residual amounts of *PPH1* mRNA (Fig. S5).

Figure 2. PPH1 is a chloroplast protein
(A) *In vitro* import into Arabidopsis chloroplasts. Radio-labelled PPH1 precursor obtained by *in vitro* translation was incubated for the indicated times with chloroplasts isolated from Arabidopsis leaves. After the incubation, an aliquot was treated with thermolysin (TLysin) as specified. The proteins were extracted and analyzed by SDS-PAGE and phosphorimaging.
(B) *In vitro* import into pea chloroplasts.
(C) Transient expression of PPH1::GFP in tobacco. *Nicotiana benthamiana* leaves were infiltrated with Agrobacterium containing the *35S::PPH1::GFP* construct. After two days, protoplasts were isolated and observed under the confocal microscope. The four columns show chlorophyll autofluorescence, GFP fluorescence, merged images of the two, and transmission images.
(D) Non-transformed protoplast as negative control.

Figure 3. Localization of PPH1 in chloroplast sub-fractions
(A) Immunoblot analysis of proteins from intact chloroplasts, membrane fraction (thylakoids) and soluble fraction (stroma) of chloroplasts isolated from wild-type (WT) and *pph1-1* plants with antibody against PPH1. Antibodies against reference proteins were used as controls for the stromal (Rubisco) and thylakoid (Lhcb1) fractions. The samples contained 1 µg of chlorophyll for the chloroplast and thylakoid samples, and 1.5 µg of protein for the stroma.
(B) Immunoblot analysis of thylakoid membrane subfractions (Tk: thylakoids; G+M: grana + margins; SL: stroma lamellae) isolated from wild-type plants with antibody against PPH1. The lower panels show immunodetection with antibodies against the D1 subunit of PSII and the PsaF subunit of PSI. Loading of the samples was on an equal chlorophyll basis (1 µg for PPH1 and 0.2 µg for D1 and PsaF).

Figure 4. Analysis of state transitions
(A) Chlorophyll fluorescence emission spectra at low temperature. Rosette leaves from Col0 wild type, three *pph1* alleles and *stn7* grown in short days under white light were treated for 30 min under far-red (state 1 conditions) or blue light (state 2 conditions). Crude extracts were frozen in liquid nitrogen and fluorescence emission spectra were obtained with excitation at 480 nm. The curves were normalized for the PSII peak at 685 nm (average of 4 measurements). The fluorescence emission peak from PSI was at approximately 732 nm.
(B) Chlorophyll fluorescence analysis at room temperature. State transitions were measured with a PAM chlorophyll fluorimeter to monitor changes in the light-harvesting antenna associated with PSII. A dark-adapted leaf was exposed to blue light to induce state 2, then with additional far-red light to promote a transition to state 1, and was induced to return to state 2 after the far-red light was switched off. State transitions were estimated as the difference in maximal fluorescence in state 1 (Fm1) and in state 2 (Fm2), which was abolished in *stn7*, strongly reduced in *pph1-1* and barely detectable in *pph1-2*. State transitions are also denoted by small changes in fluorescence when the lights are switched. These reflect changes in the redox state of the plastoquinone pool. In *stn7*, where the LHCII antenna stayed associated with PSII in blue light and the plastoquinone pool remained reduced, the decrease in fluorescence when the far-red light was turned on was more pronounced than in the wild type, where the state transition led to a gradual oxidation of the plastoquinone pool in blue light. As could be expected for a phosphatase mutant which favors state 2, only minor fluorescence changes were observed in *pph1-1* and *pph1-2* because the plastoquinone pool stayed predominantly oxidized.
(C) Quantification of state transitions measured as in panel (B): $qT = (F_{m1}-F_{m2})/F_{m1} \times 100$ (average of 4 different leaves, mean +/- SD).

Table Legends

Table 1. Mass-spectrometric quantification of thylakoid protein phosphorylation
The sequence of the peptides is indicated with their modifications: Ac, N-terminal acetyl group; lower case t, phosphorylated threonine residue. The mutant / wild type ratios were determined in every LC-MS experiment from the areas of extracted ion chromatograms for each of the differentially labeled phosphorylated peptides corresponding to a particular protein. The data are averages (+/- SD) from four different experiments.
(*) The Ac-RRtVK phosphopeptide signal was not detected in the wild-type sample in three experiments.

Table 1

	Phosphopeptide sequence	Protein names	At gene identifier	Mutant / wild type ratio
LHCII	Ac-RKtVAKPK	LHCB1.1 LHCB1.2 LHCB1.3 LHB1B2 (LHCB1.5)	At1g29910 At1g29920 At1g29930 At2g34420	3.6 +/- 0.2
	Ac-RRtVK	LHCB2.1 LHCB2.2 LHCB2.4	At2g05100 At2g05070 At3g27690	> 13 (*)
PSII core	Ac-tAILER	D1	AtCg00020	1.1 +/- 0.2
	Ac-tIALGK	D2	AtCg00270	1.5 +/- 0.3

Figure 1

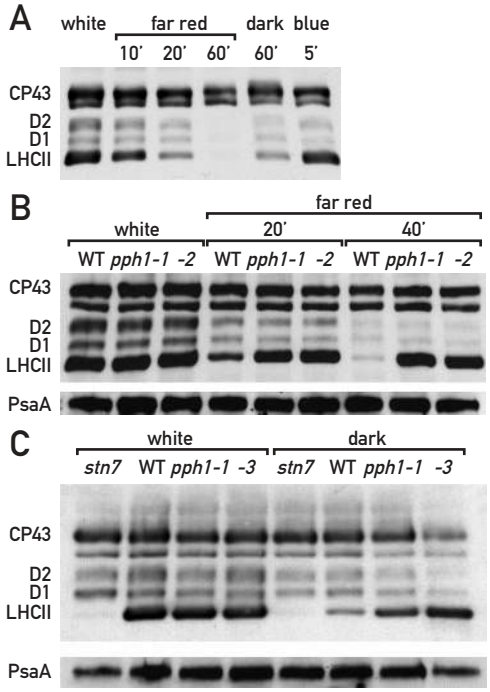
A
white
far red
dark
blue
10'
20'
60'
60'
5'
CP43
D2
D1
LHCII
B
far red
white
20'
40'
WT pph1-1 -2
WT pph1-1 -2
WT pph1-1 -2
CP43
D2
D1
LHCII
PsaA
C
white
dark
stn7
WT pph1-1 -3
stn7
WT pph1-1 -3
CP43
D2
D1
LHCII
PsaA

Figure 2

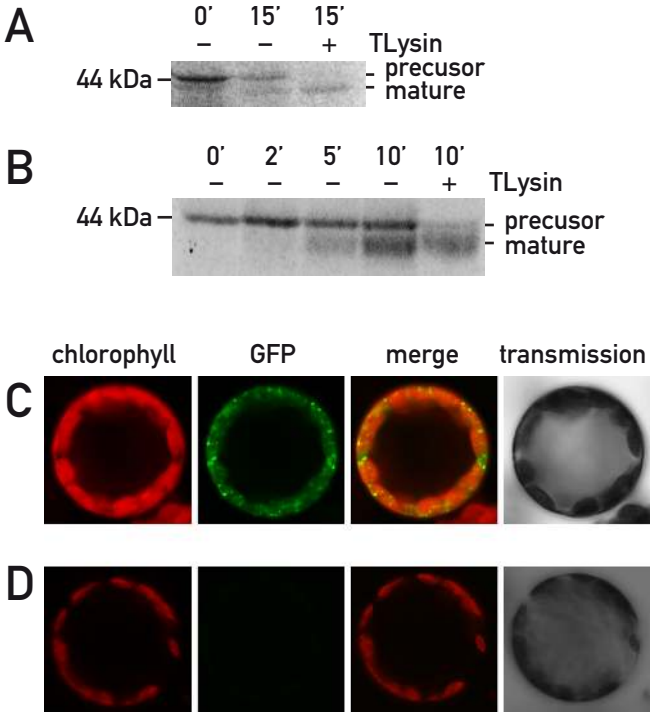
A
0'
15'
15'
–
–
+
TLysin
44 kDa
precusor
mature
B
0'
2'
5'
10'
10'
–
–
–
–
+
TLysin
44 kDa
precusor
mature
chlorophyll
GFP
merge
transmission
C
D

Figure 3

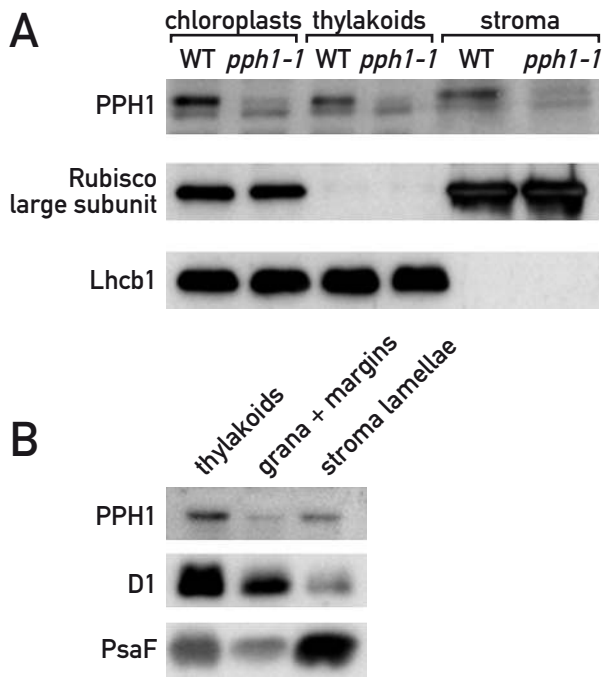
A
chloroplasts
thylakoids
stroma
WT
pph1-1
WT
pph1-1
WT
pph1-1
PPH1
Rubisco
large subunit
Lhcb1
B
thylakoids
grana + margins
stroma lamellae
PPH1
D1
PsaF

Figure 4

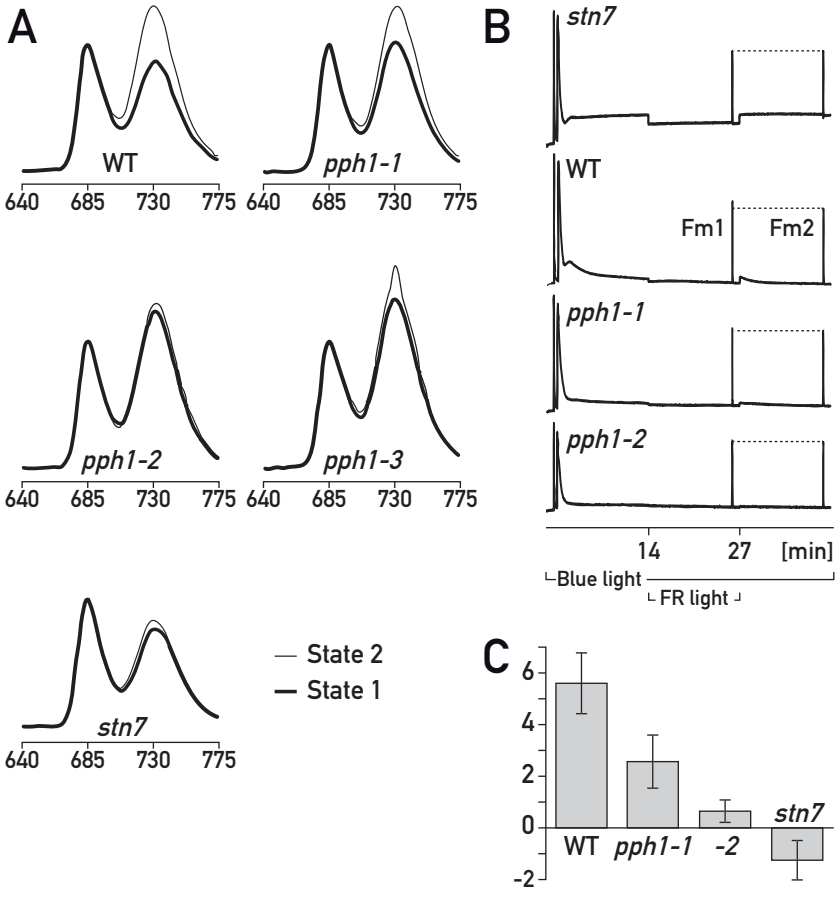
A
WT
pph1-1
pph1-2
pph1-3
stn7
640
685
730
775
State 2
State 1
B
stn7
WT
Fm1
Fm2
pph1-1
pph1-2
14
27
[min]
Blue light
FR light
C
6
4
2
0
-2
WT
pph1-1
-2
stn7

Supporting Information.

Figure S1. Mass-spectrometric analysis of thylakoid protein dephosphorylation

(A) Extracted ion chromatograms of the phosphorylated peptides from the *pph1-1* mutant labeled with heavy isotope (dashed line) and the wild type labeled with light isotope (solid line) analyzed by LC-MS. The peaks corresponding to two N-terminal peptides from LHCII and to two N-terminal peptides from PSII (D1 and D2) are marked. The tandem MS fragmentation spectra of all phosphorylated peptides are presented in Figures S2 and S3.

(B) Extracted ion chromatograms from the reciprocal labeling experiment where peptides from the *pph1-1* mutant were labeled with light isotope (solid line) and peptides from wild type were labeled with heavy isotope (dashed line).

Figure S2. Tandem MS fragmentation spectra of the LHCII peptides Ac-RRtVK and Ac-RKtVAKPK

(A-D) Collision-induced dissociation (CID) and Electron transfer dissociation (ETD) fragmentation spectra of the acetylated N-terminal phosphopeptide RRtVK present in LHCB2.1 (At2g05100), LHCB2.2 (At2g05070) and LHCB2.4 (At3g27690). Lower case t: phosphorylated threonine residue. The positions of b,c (N-terminal) and z,y (C-terminal) fragment ions are indicated in the spectra.

(A) CID and (B) ETD fragmentation spectra of the selected doubly protonated parent ion with m/z 398.2 corresponding to the Ac-RRtVK peptide labeled with light stable isotope.

(C) CID and (D) ETD fragmentation spectra of the selected doubly protonated parent ion with m/z 399.7 corresponding to the Ac-RRtVK peptide labeled with heavy stable isotope.

(E-H) CID and ETD fragmentation spectra of the acetylated N-terminal phosphopeptide Ac-RKtVAKPK present in LHCB1.1 (At1g29910), LHCB1.2 (At1g29920), LHCB1.3 (At1g29930) and LHB1B2 (LHCB1.5; At2g34420).

(E) CID and (F) ETD fragmentation spectra of the selected doubly protonated parent ion with m/z 532.3 corresponding to the Ac-RKtVAKPK peptide labeled with light stable isotope.

(G) CID and (H) ETD fragmentation spectra of the selected doubly protonated parent ion with m/z 533.8 corresponding to the Ac-RKtVAKPK peptide labeled with heavy stable isotope. The positions of b,c (N-terminal) and z,y (C-terminal) fragment ions are indicated in the spectra.

Figure S3. **Tandem MS fragmentation spectra of the photosystem II peptides Ac-tIALGK and Ac-tAILER**

(A and B) CID fragmentation spectra of the acetylated N-terminal phosphopeptides tIALGK corresponding to D2 protein and tAILER corresponding to D1 protein of photosystem II. Lower case t: phosphorylated threonine residue. The positions of y (C-terminal) and b (N-terminal) fragment ions are indicated in the spectrum.

(A) CID fragmentation spectra of the selected singly protonated parent ion with m/z 738.4 corresponding to Ac-tIALGK labeled with light stable isotope.
(B) CID fragmentation spectra of the selected singly protonated parent ion with m/z 741.4 corresponding to Ac-tIALGK labeled with heavy stable isotope.

(C and D) CID fragmentation spectra of the acetylated N-terminal phosphopeptide tAILER corresponding to D1 protein of photosystem II.
(C) CID fragmentation spectra of the selected singly protonated parent ion with m/z 852.4 corresponding to Ac-tAILER labeled with the light stable isotope.
(D) CID fragmentation spectra of the selected singly protonated parent ion with m/z 858.4 corresponding to Ac-tAILER labeled with the heavy stable isotope.

Figure S4. Structure of the PPH1 gene
The two alternative spliced forms of the *PPH1* mRNA are depicted with their exons (boxes) and introns (thin lines). The 5'UTR and 3'UTR are shown in white. The positions of the T-DNA insertions in three mutant lines are indicated with triangles. The oligonucleotides used for Reverse Transcription - PCR are depicted with arrows.
The two predicted isoforms of PPH1 are represented with the phosphatase domain in light grey and the putative transmembrane domain in orange. Eleven motifs which are conserved in PP2C phosphatases are shown with asterisks (1). A domain which is characteristic of PPH1 and its orthologues in other plants is shown blue.

Figure S5. Analysis of *PPH1* mRNA
(A) Reverse Transcription - PCR. RNA from mature leaves was subjected to RT-PCR with the oligonucleotides shown in Figure S4. The bands were extracted from the gel and analyzed by sequencing. The upper band corresponds to At4g27800.2, the lower band to At4g27800.1.

(B) RNA blots of transcripts from the wild type, three *pph1* alleles and *stn7* were probed with *PPH1* and then with actin as a control. The bottom panel shows total RNA stained with ethidium bromide. For quantitative comparison, different amounts of wild-type RNA were loaded as indicated.

Figure S6. Phylogenetic analysis of *PPH1*
The tree was derived for all the predicted PP2C phosphatases of Arabidopsis (2) as well as top-scoring homologs of *PPH1* (AT4G27800) from other species identified in a BLAST search, using the ClustalW (3) and displayed with Dendroscope (4). Surprisingly, whereas Stt7 is definitely the ortholog of STN7 in Chlamydomonas (5), we could not detect a clear orthologue for PPH1.

MATERIALS AND METHODS

Plant genotyping

T-DNA insertions were analyzed by PCR using combinations of the following primers: (a) for SALK_025713C: LBa1, 5'- TGG TTC ACG TAG TGG GCC ATC G; R (reverse primer), 5'- GAG GAA TTT GAC AGA GGA CGA C; F (forward primer), 5'-GGA ACA TCT TAA TTC TTA AAT GAA GG (b) for line SAIL_514-C03: LB, 5'-TTC ATA ACC AAT CTC GAT ACA C; F; R (c) for GABI_232H12 line: sail08409, 5'-ATA TTG ACC ATC ATA CTC ATT GC; H12-F, 5'-CTC ATA TTG GTG ATT CGT GTG C; H12-R, 5'-AGC AAT GAA TCG GTT TTA AGC C.

Analysis of *in vivo* protein phosphorylation in *pph1-1* by mass spectrometry

To identify proteins which remain phosphorylated in the mutant plants exposed to far-red light we used the approach of differential stable isotope labeling and mass spectrometry. Wild-type and mutant *pph1-1* seedlings were exposed to far-red light for 30 minutes, and thylakoid membranes were isolated in the presence of NaF that inhibits dephosphorylation of thylakoid proteins (6). The isolated thylakoids were resuspended to equal chlorophyll concentration and subjected to proteolytic shaving of the surface-exposed phosphopeptides from the membranes by trypsin (7). The released peptide mixtures were separated from the rest of the membranes by centrifugation.

Preparation of Peptide Methyl Esters

The tryptic peptides from the wild type thylakoids were esterified with d_0-methanol (modification of each carboxyl group gives a peptide mass increment of 14 Da), while the peptides from the mutant thylakoids were esterified with d_3-methanol (modification of each carboxyl group gives a peptide mass increment of 17 Da). Peptides were methyl esterified essentially as described in (8). Shortly, lyophilized peptides obtained by trypsinolysis of thylakoids that contained 40µg of chlorophyll were methyl-esterified with either 200 µL of 2 N methanolic HCl or DCl prepared by addition of 160 µL of acetylchloride to 1mL of anhydrous d_0-methyl alcohol or to 1mL of anhydrous d_3-methyl d-alcohol (both Sigma-Aldrich). The reaction was carried out at room temperature for 3h followed by lyophilisation and one additional round of methyl-esterification before the lyophilized samples were reconstituted with 10 µL 0.1 % (v/v) acetic acid in methanol, acetonitrile, water (1:1:1). Light-isotope labeled peptides from wild type thylakoids were mixed 1:1 with heavy-isotope labeled peptides from *pph1-1* thylakoids prior to phosphopeptide enrichment. We also performed the reverse labeling of the wild type and mutant peptides as an internal control.

Phosphopeptide Enrichment

Phosphopeptides were enriched by the IMAC method as described (8, 9). Chelating Sepharose (15 µL, Amersham Biosciences) was prepared in GELoader tips (Eppendorf) and loaded with 120 µL of 0.1 M $FeCl_3$ followed by a wash with 90 µL 0.1 % acetic acid to remove unbound iron ions. Differentially methyl-esterified samples were mixed 1:1 and loaded on the column. The column was washed with 30 µL of 0.1 % acetic acid followed by an additional wash with 120 µL of 0.1 % acetic acid in 20 % acetonitrile.

Bound phosphopeptides were eluted by addition of 120 µL 20mM Na_2HPO_4 in 20 % acetonitrile.
The phosphorylated peptides enriched by each round of IMAC were analyzed by nano-liquid chromatography (LC) electrospray ionization mass spectrometry (MS) in positive ionization mode, which allowed simultaneous measurements of intensities for light- and heavy-isotope labeled phosphopeptide pairs and quantitative comparison of the phosphorylation differences in the mutant and wild-type proteins. For analysis of the peptides an on-line nano-flow HPLC system (EASY-nLC from Bruker Daltonics, Bremen, Germany) and MS analysis using HCTultra PTM Discovery System (Bruker Daltonics, Bremen, Germany) was performed. A 20 mm x 100 µm pre column followed by a 100 mm x 5 µm column, both reverse phase C18 material with particle size 5 µm 120 Å, were used for separation at a flow rate of 300 nL/min in a gradient from 0.1 % formic acid in water to 0.1 % formic acid in 100 % acetonitrile. The separation was performed for 90 min ([t (min), % acetonitrile]: [0-5, 0-3] [5-40, 3-7] [40-65, 7-30] [65-75, 30-100] [75-90, 100]). The automated online tandem MS analyses were made using alternating CID/ETD fragmentation of peptide ions.

RT-PCR, RNA blotting

For reverse transcription - PCR (RT-PCR), RNA was isolated using RNeasy Plant Mini Kit (Quiagen) according to manufacturers' protocol. First strand cDNA was synthesized with the SuperScript II system (Invitrogen) using gene-specific primers. To discriminate between the three possible splice variants of *PPH1* cDNA was subjected to PCR with two pairs of primers: PPH1(1,2)-F: 5'-GAA ACA TGG GAA TGT GCA GCT and PPH1-R: 5'-GAT AGA TGT GAA GAC ATC CAT ATG CC to reveal the two longer splice forms, or PPH1(3)-F: 5'-GAA ACA TGG GAA TGT GCA GGC with the same reverse primer to amplify the shortest splice form.
For RNA blotting, total RNA was isolated using TRI-reagent (Sigma-Aldrich) and separated in formaldehyde/MOPS agarose gel (30 µg/lane). RNA was blotted to nylon membrane (Hybond N+; GE Healthcare) by upward capillary transfer using 10 x SSC as transfer buffer, and immobilized by UV crosslinking. The membrane was hybridized with a ^{32}P-labeled *PPH1* cDNA probe or an actin probe as control as described (10).

Localization of PPH1::GFP in tobacco

DNA vector for plant transformation

The complete coding sequence of PPH1 (At4g27800), excluding the stop codon, was amplified by PCR from a cDNA clone (pda07463) obtained from the Riken Institute. Forward (5'- TCT AGA ATG GCG CTT CTG AG) and reverse (5'- CTC GAG AGA TAG ATG TGA AGA CAT CCA) primers included XbaI and XhoI sites, respectively. The PCR product was ligated in the XbaI and XhoI sites of p19-EGFP (kindly donated by Dr. K.P. Lee from University of Geneva, Switzerland), resulting in C-terminal GFP fusion under the control of the CaMV 35S promoter and the NOS terminator.

Detection of PPH1::GFP fusion protein

Leaves of *Nicotiana benthamiana* were infiltrated using *Agrobacterium tumefaciens*, GV 3101 strain, and infiltration buffer (10 mM MES; 10 mM $MgCl_2$; 150 µM

acetosyringone). After 48 h, protoplasts were isolated as described (11) and fluorescence was monitored using a laser scanning confocal microscope. GFP was detected using the FITC (488 nm) laser line from a LEICA TCS 4D microscope (LEICA Microsystems). Leica Lite software release 2.61 and Adobe Photoshop 7 (Adobe Systems, San Jose, CA) were used for image acquisition and processing, respectively.

Chlorophyll fluorescence measurements at 77 K

Detached rosette leaves from short day-grown plants floating on distilled water in Petri dishes were placed under panels of far-red or blue LED lamps (L735 and L470, respectively; Epitex, Kyoto, Japan) for 30 min to induce state 1 or state 2. Then leaves were briefly wiped dry and snap-frozen in liquid nitrogen. The samples were ground 4 x 10 s in a triturator (Silamat S5; Ivoclar Vivadent AG, Schaan, Liechtenstein) using pre-cooled glass beads. To the frozen powder 700 µL of ice-cold buffer containing 50 mM Hepes-KOH, pH 7.5, 100 mM sorbitol, 10 mM $MgCl_2$, and 10 mM NaF was added, the sample was rapidly mixed and filtered through a syringe-based porous filter unit. The cleared filtrate was loaded into a capillary and frozen in liquid nitrogen. Chlorophyll fluorescence at 77 K was recorded on a Jasco FP-750 spectrofluorometer. Excitation was at 480 nm (slit width 5 nm) and emission was recorded in the 600-800 nm range (slit width 5 nm). The curves were normalized for the PSII peak at 685 nm.

Chlorophyll fluorescence analysis at room temperature

Plants grown in short days were taken 2 h after the onset of the light period and transferred to the dark. After 1 h a leaf was detached and placed into a sample clip over a piece of wet filter paper to prevent desiccation. Chlorophyll fluorescence profiles were recorded using an FMS1 Pulse Modulated Fluorimeter (Hansatech; Norfolk, England) as described previously (12, 13) with the following protocol: t = 0, measuring beam on; t = 1 min, saturating flash; t = 1.5 min, blue light on; t = 15.5 min, far-red light on; t = 27.5 min, saturating flash; t = 28.5 min, far-red light off; t = 40.5 min, saturating flash; t = 41.5 min, blue light off.

References

1. Bork P, Brown NP, Hegyi H, & Schultz J (1996) The protein phosphatase 2C (PP2C) superfamily: detection of bacterial homologues. *Protein Sci* 5:1421-1425.
2. Kerk D, Templeton G, & Moorhead GB (2008) Evolutionary radiation pattern of novel protein phosphatases revealed by analysis of protein data from the completely sequenced genomes of humans, green algae, and higher plants. *Plant Physiol* 146:351-367.
3. Larkin MA*, et al.* (2007) Clustal W and Clustal X version 2.0. *Bioinformatics* 23:2947-2948.
4. Huson DH*, et al.* (2007) Dendroscope: An interactive viewer for large phylogenetic trees. *BMC Bioinformatics* 8:460.
5. Depege N, Bellafiore S, & Rochaix JD (2003) Role of chloroplast protein kinase Stt7 in LHCII phosphorylation and state transition in Chlamydomonas. *Science* 299:1572-1575.

6. Vener AV, Rokka A, Fulgosi H, Andersson B, & Herrmann RG (1999) A cyclophilin-regulated PP2A-like protein phosphatase in thylakoid membranes of plant chloroplasts. *Biochemistry* 38:14955-14965.
7. Vener AV, Harms A, Sussman MR, & Vierstra RD (2001) Mass spectrometric resolution of reversible protein phosphorylation in photosynthetic membranes of Arabidopsis thaliana. *J Biol Chem* 276:6959-6966.
8. Vainonen JP, Hansson M, & Vener AV (2005) STN8 protein kinase in Arabidopsis thaliana is specific in phosphorylation of photosystem II core proteins. *J Biol Chem* 280:33679-33686.
9. Ficarro SB*, et al.* (2002) Phosphoproteome analysis by mass spectrometry and its application to Saccharomyces cerevisiae. *Nat Biotechnol* 20:301-305.
10. Goldschmidt-Clermont M (1986) The two genes for the small subunit of RuBP carboxylase/oxygenase are closely linked in Chlamydomonas reinhardtii. *Plant Molecular Biology* 6:13-21.
11. Vidi PA, Kessler F, & Brehelin C (2007) Plastoglobules: a new address for targeting recombinant proteins in the chloroplast. *BMC Biotechnol* 7:4.
12. Bellafiore S, Barneche F, Peltier G, & Rochaix JD (2005) State transitions and light adaptation require chloroplast thylakoid protein kinase STN7. *Nature* 433:892-895.
13. Lunde C, Jensen PE, Haldrup A, Knoetzel J, & Scheller HV (2000) The PSI-H subunit of photosystem I is essential for state transitions in plant photosynthesis. *Nature* 408:613-615.

A

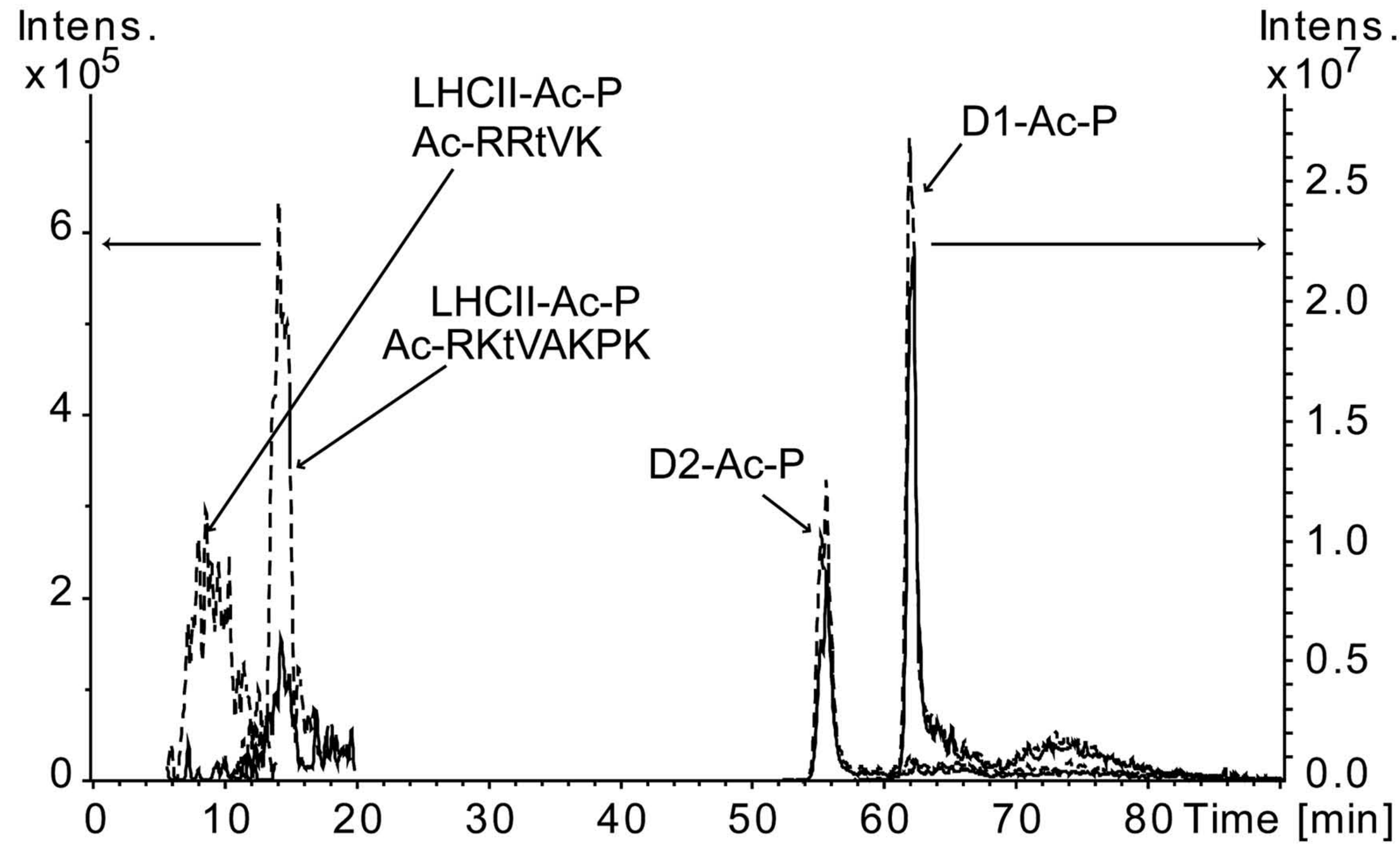

(—) Wild type light
(---) *pph1-1* heavy

B

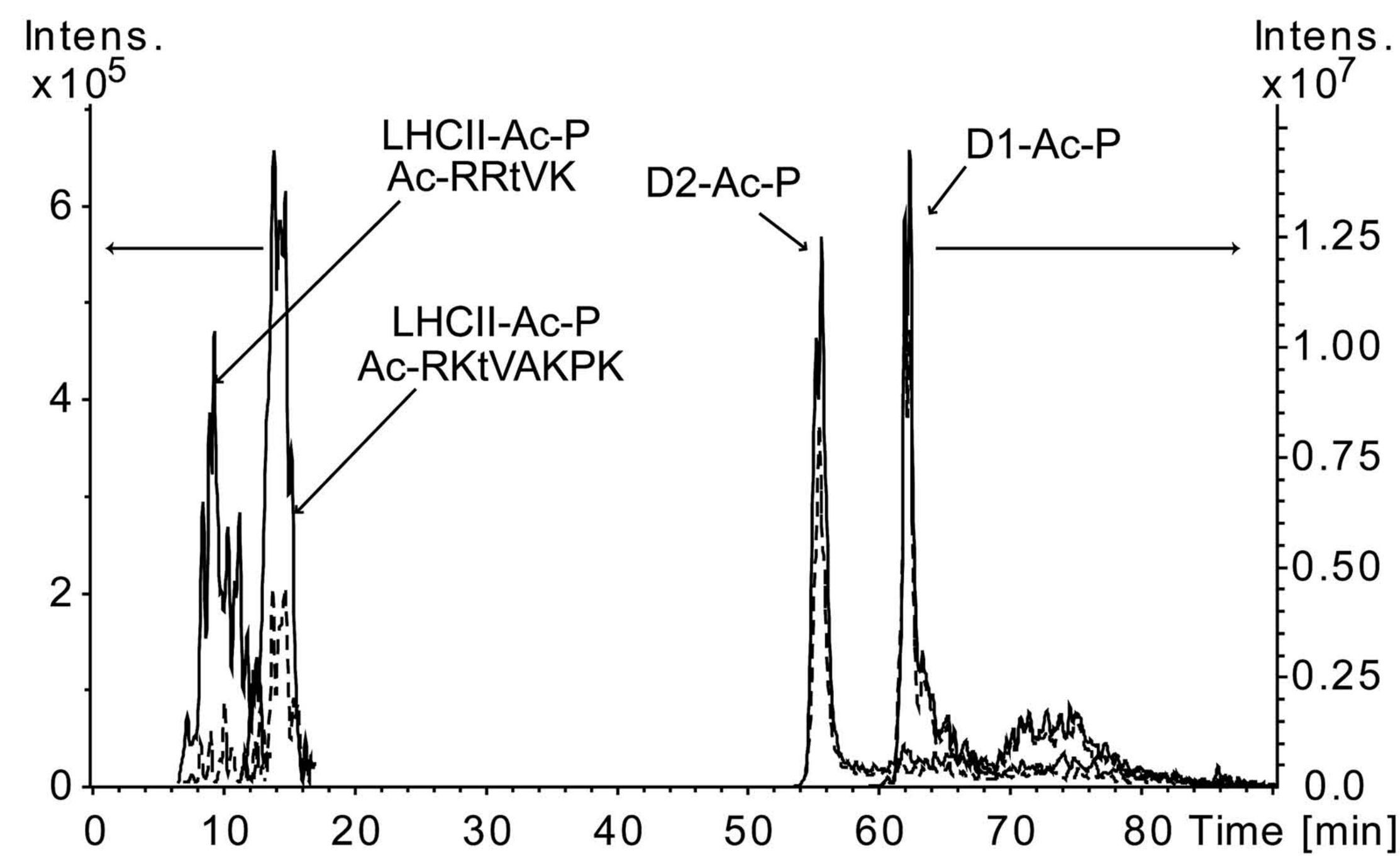

(---) Wild type heavy
(—) *pph1-1* light

A

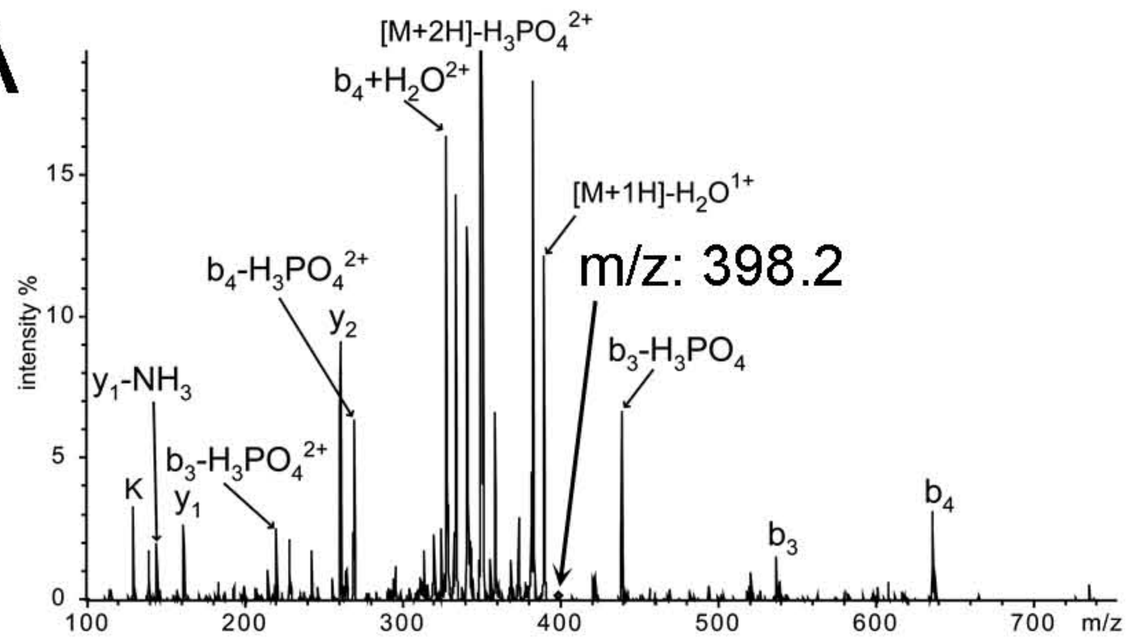
[M+2H]-H3PO4 2+
b4+H2O2+
[M+1H]-H2O1+
m/z: 398.2
b4-H3PO4 2+
y2
b3-H3PO4
y1-NH3
b3-H3PO4 2+
K
y1
b3
b4
intensity %
m/z

B

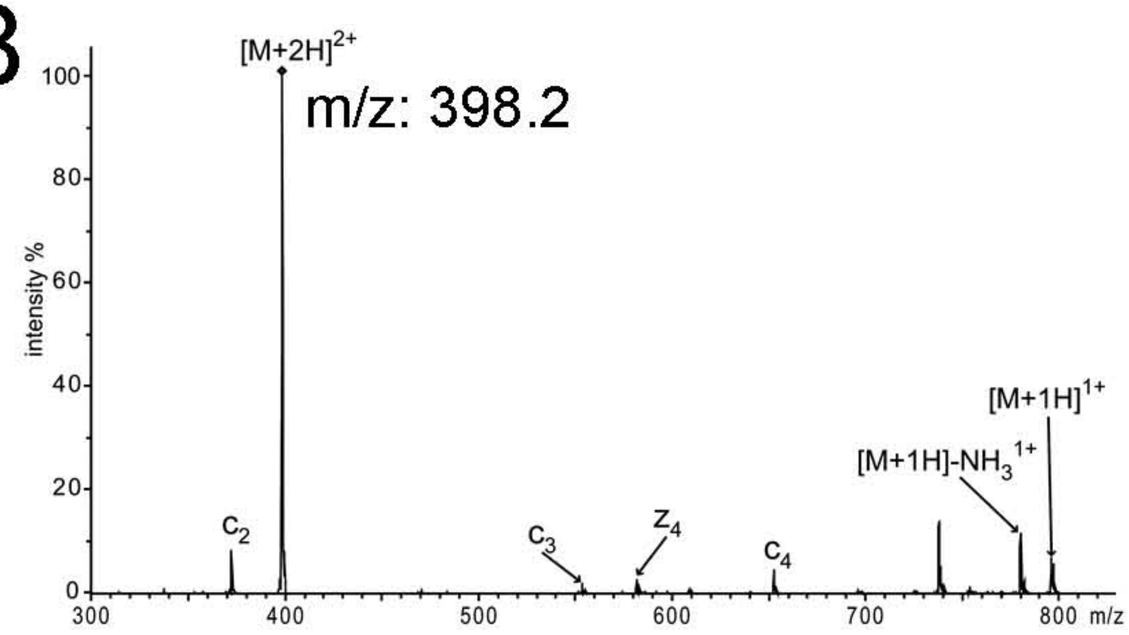
[M+2H]2+
m/z: 398.2
[M+1H]1+
[M+1H]-NH3 1+
c2
c3
z4
c4
intensity %
m/z

C

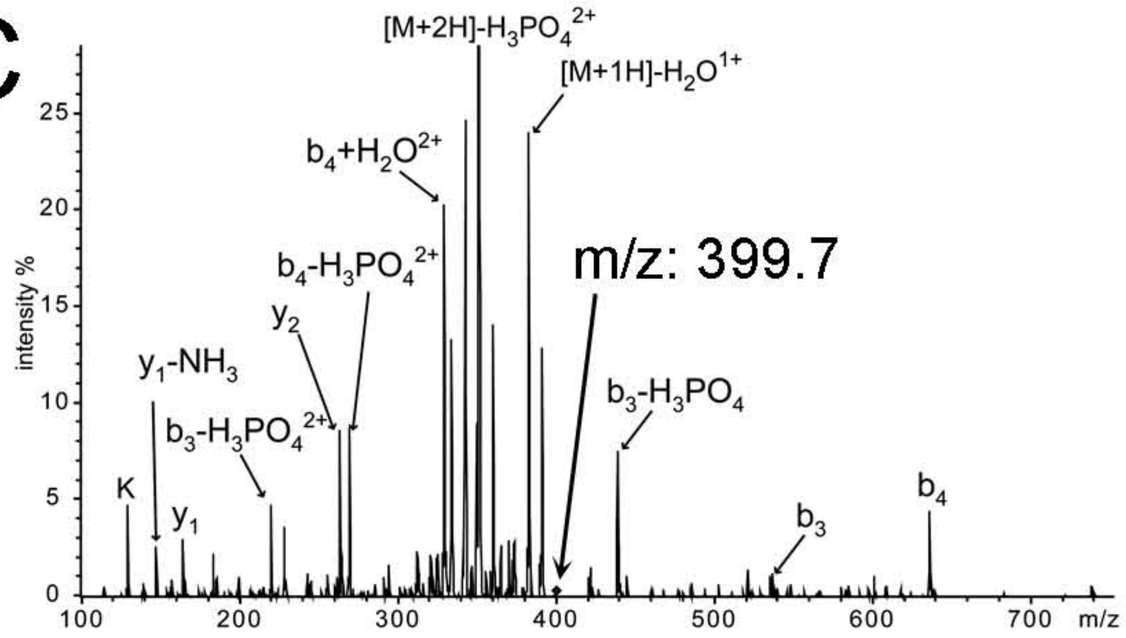
[M+2H]-H3PO4 2+
[M+1H]-H2O1+
b4+H2O2+
m/z: 399.7
b4-H3PO4 2+
y2
y1-NH3
b3-H3PO4
b3-H3PO4 2+
K
y1
b3
b4
intensity %
m/z

D

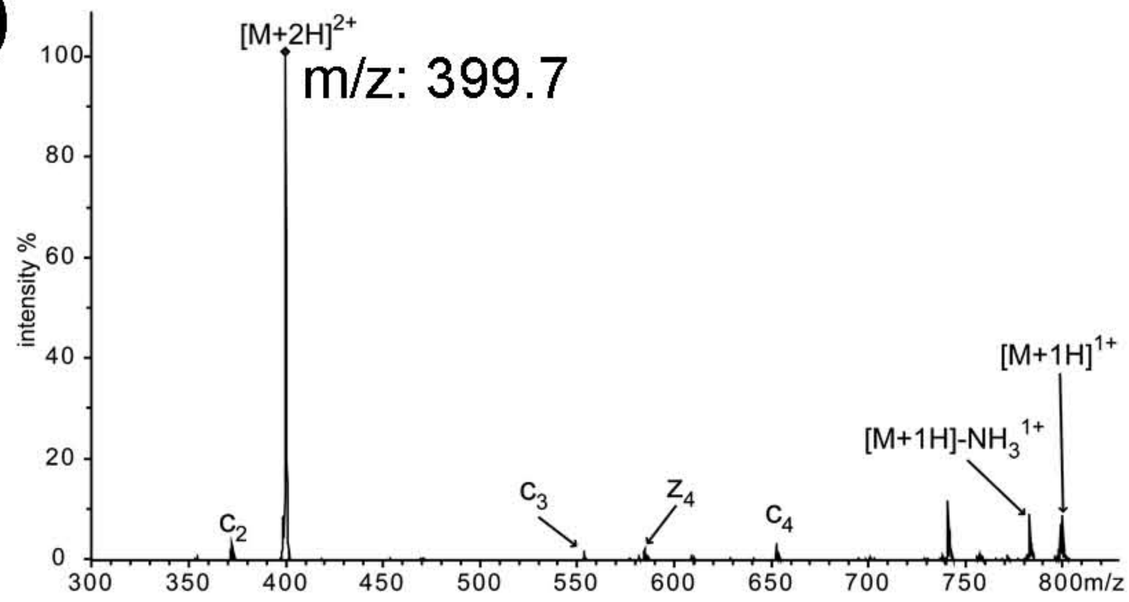
[M+2H]2+
m/z: 399.7
[M+1H]1+
[M+1H]-NH3 1+
c2
c3
z4
c4
intensity %
m/z

E

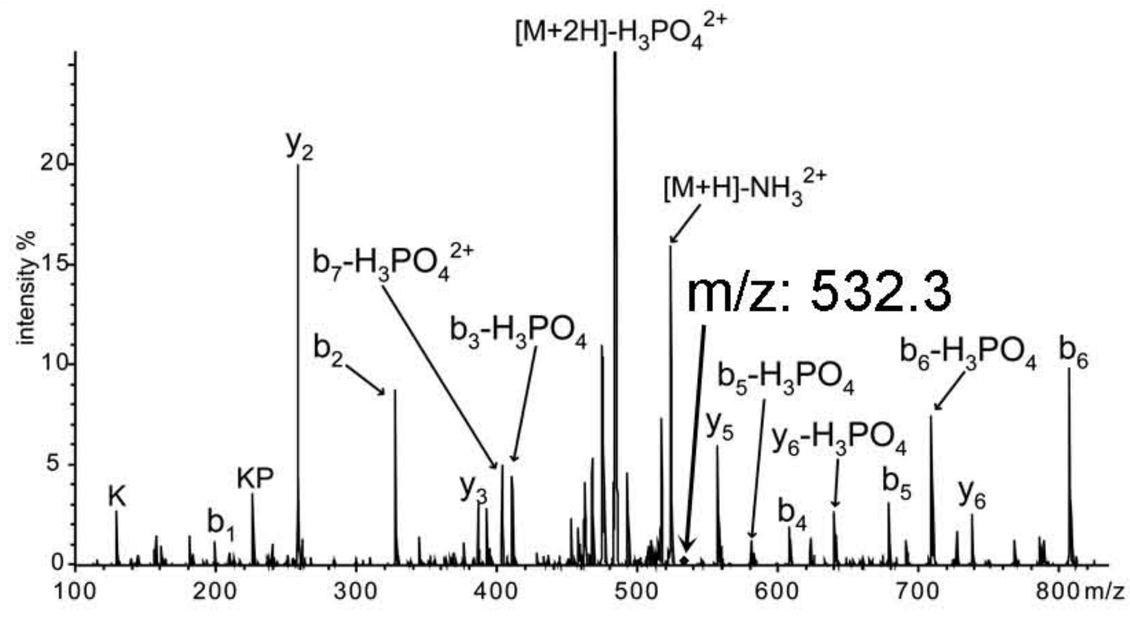
[M+2H]-H3PO4 2+
y2
[M+H]-NH3 2+
b7-H3PO4 2+
m/z: 532.3
b3-H3PO4
b2
b5-H3PO4
b6-H3PO4
b6
y5
y6-H3PO4
KP
K
b1
y3
b4
b5
y6
intensity %
m/z

F

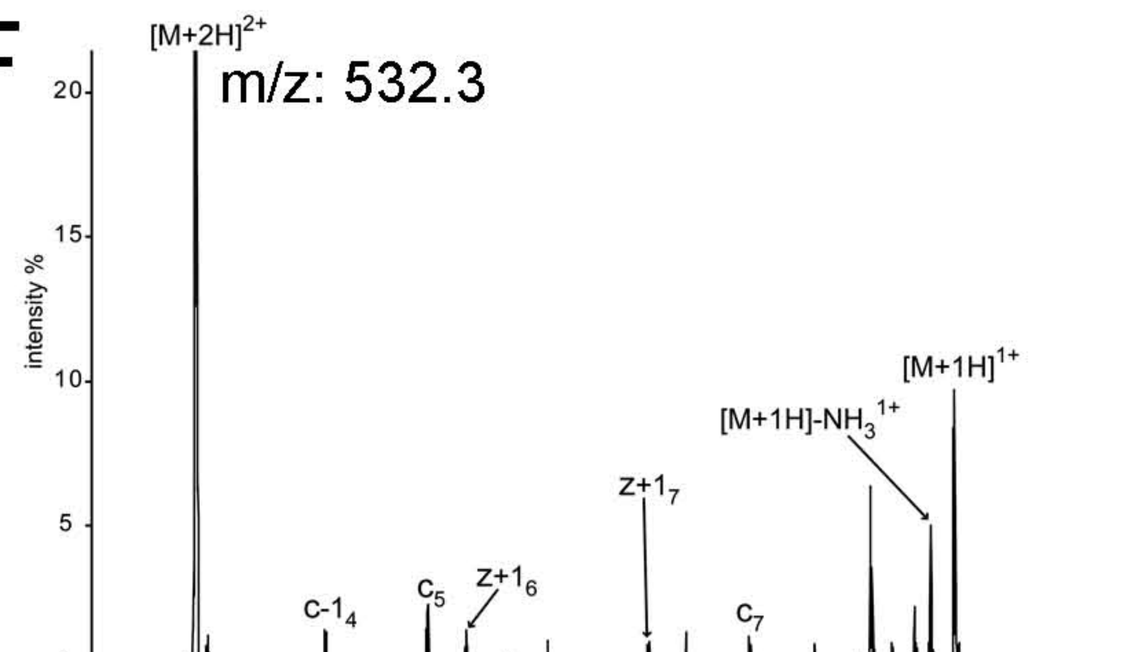
[M+2H]2+
m/z: 532.3
[M+1H]1+
[M+1H]-NH3 1+
z+17
c-14
c5
z+16
c7
intensity %
m/z

G

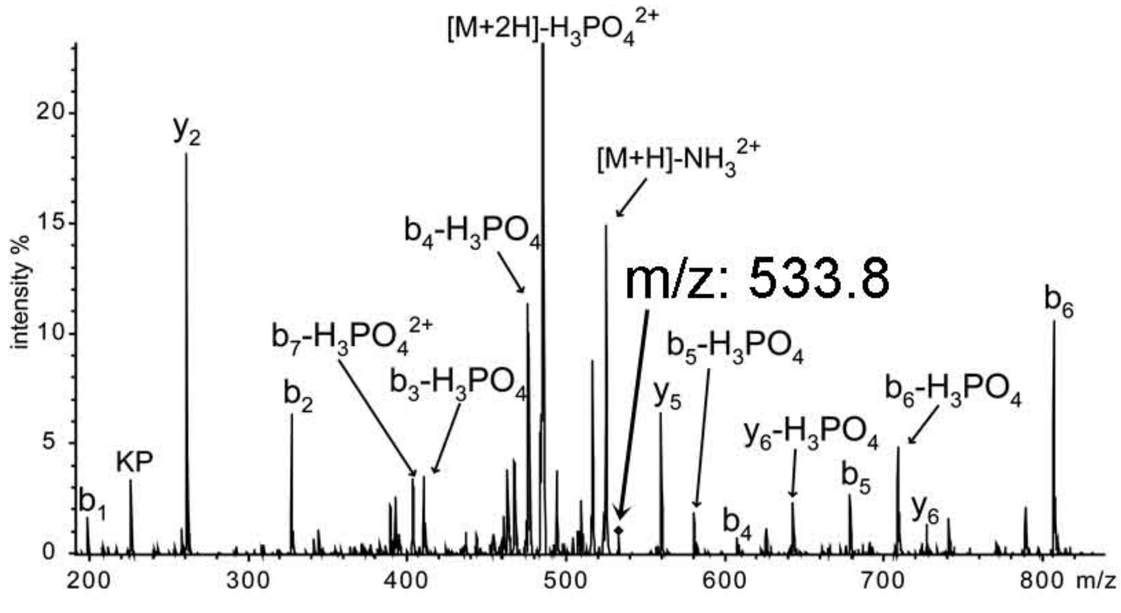
[M+2H]-H3PO4 2+
y2
[M+H]-NH3 2+
b4-H3PO4
m/z: 533.8
b7-H3PO4 2+
b5-H3PO4
b6
b2
b3-H3PO4
y5
b6-H3PO4
y6-H3PO4
KP
b1
b4
b5
y6
intensity %
m/z

H

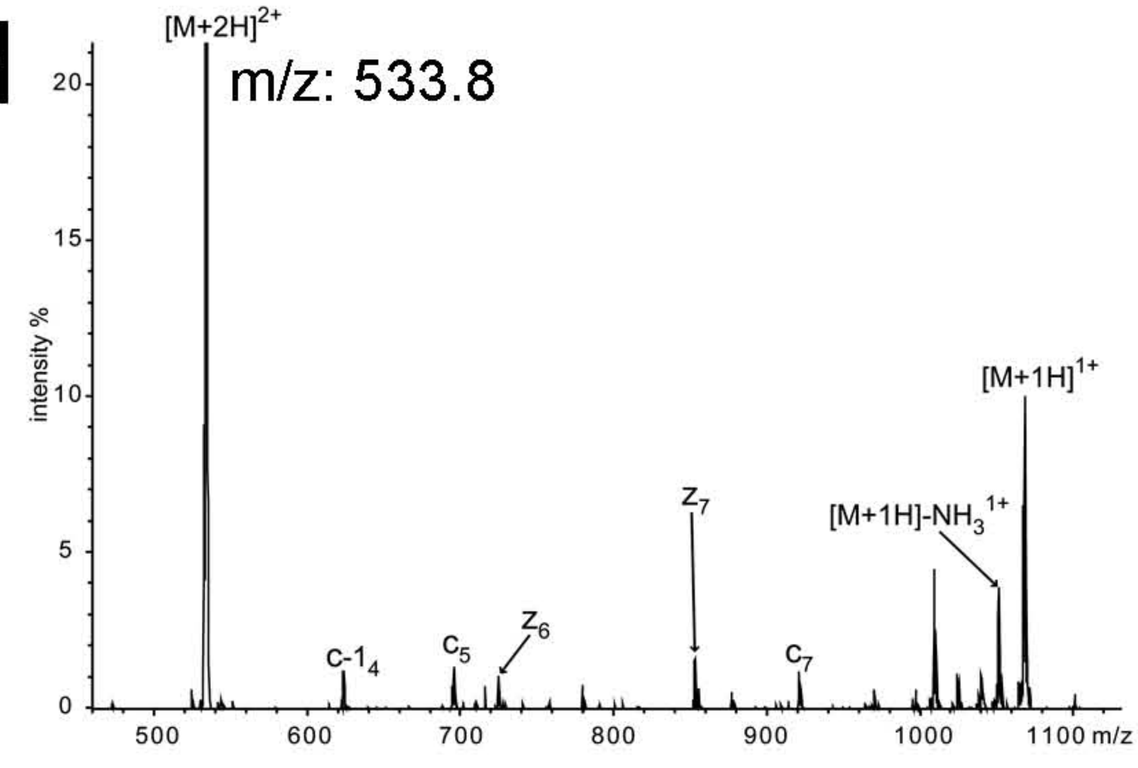
[M+2H]2+
m/z: 533.8
[M+1H]1+
[M+1H]-NH3 1+
z7
z6
c-14
c5
c7
intensity %
m/z

A

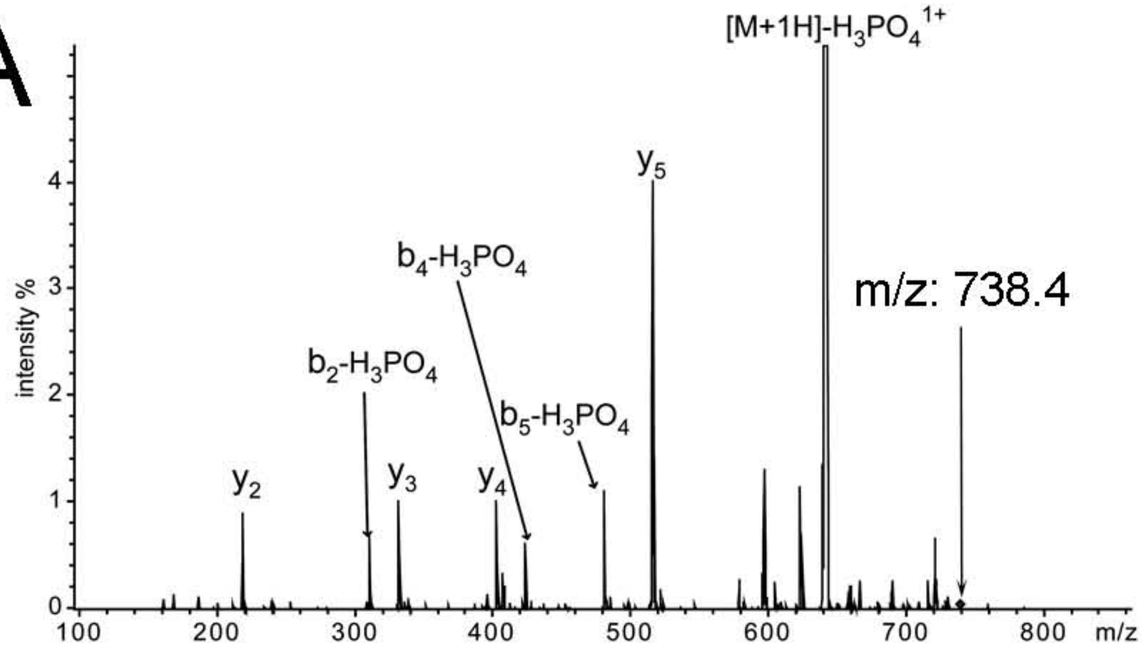
[M+1H]-H3PO4 1+
m/z: 738.4
y5
b4-H3PO4
b2-H3PO4
b5-H3PO4
y2
y3
y4
intensity %
m/z

B

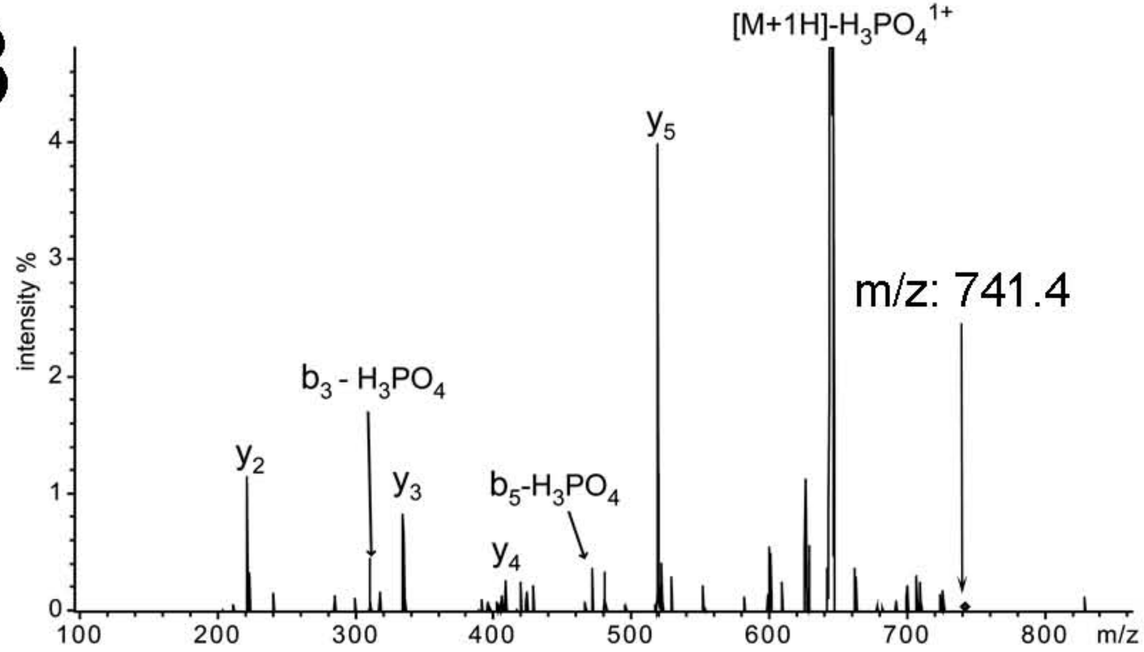
[M+1H]-H3PO4 1+
m/z: 741.4
y5
b3 - H3PO4
y2
y3
b5-H3PO4
y4
intensity %
m/z

C

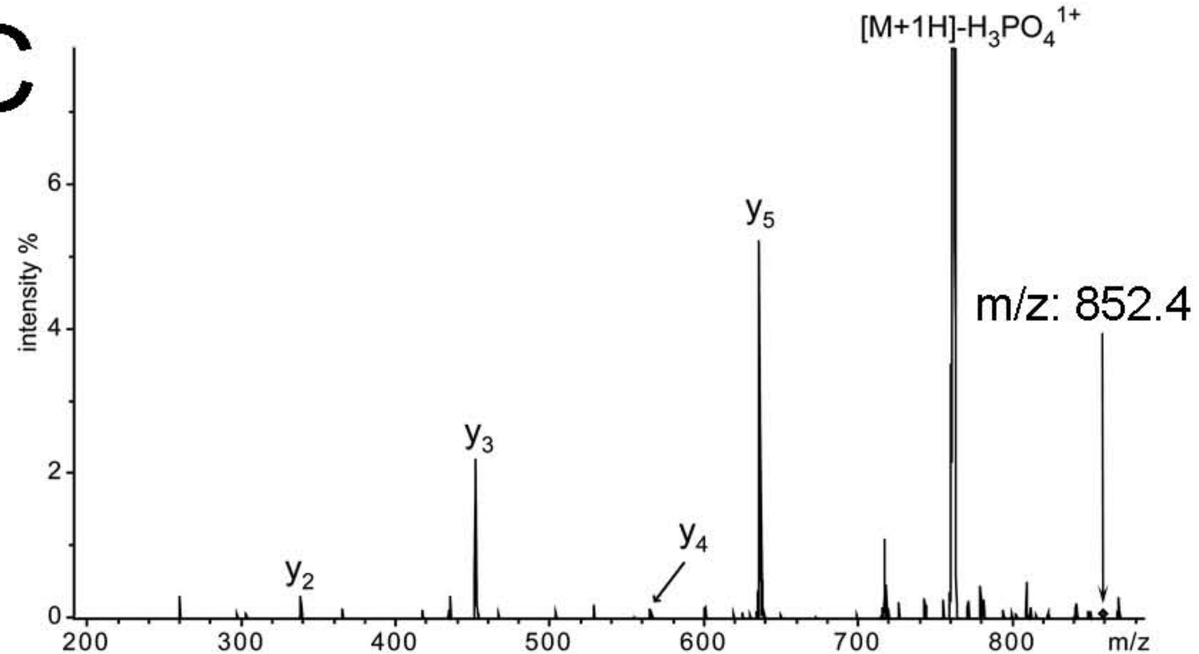
[M+1H]-H3PO4 1+
m/z: 852.4
y5
y3
y4
y2
intensity %
m/z

D

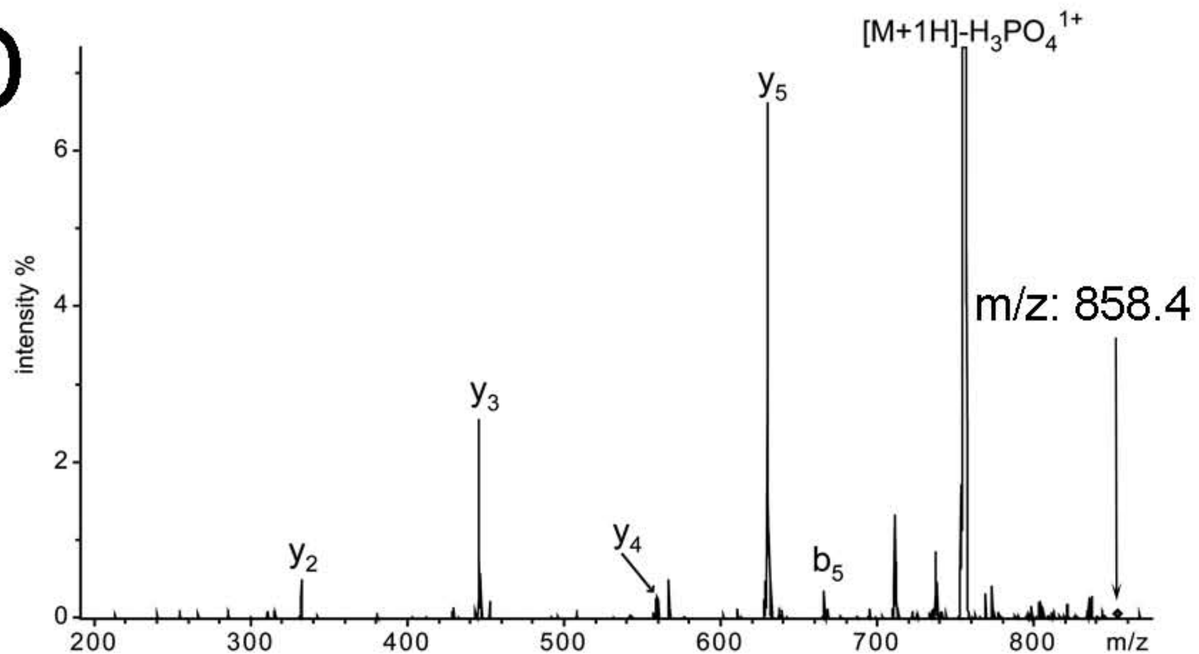
[M+1H]-H3PO4 1+
m/z: 858.4
y5
y3
y2
y4
b5
intensity %
m/z

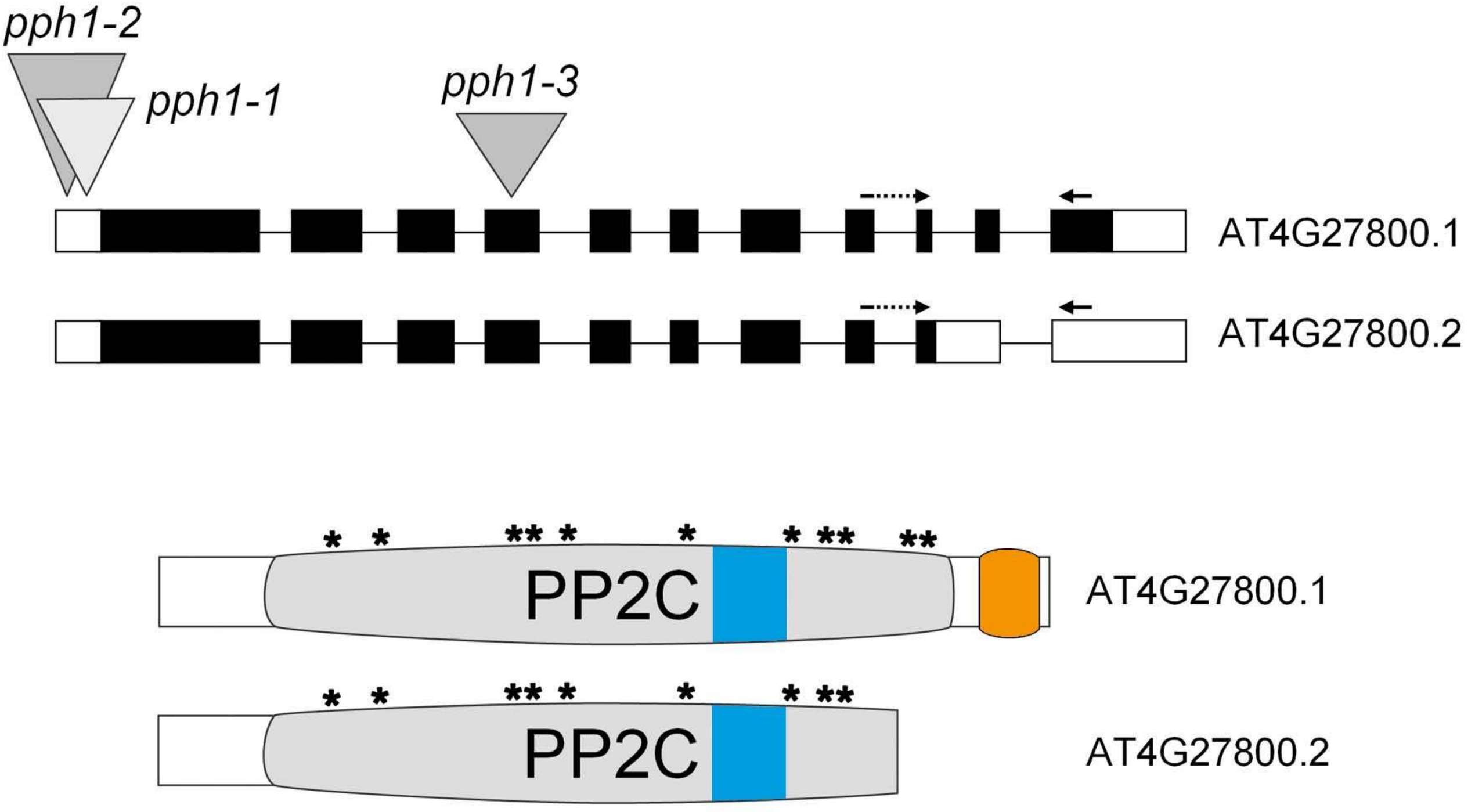
pph1-2
pph1-1
pph1-3
AT4G27800.1
AT4G27800.2
PP2C
AT4G27800.1
PP2C
AT4G27800.2

A

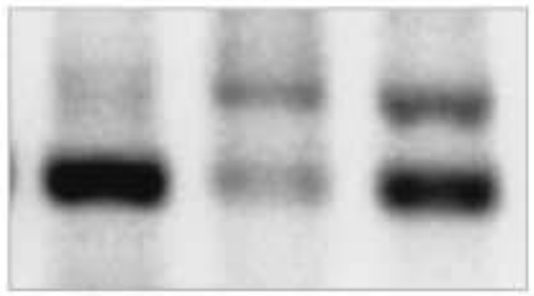
wt
pph1-1
stn7

B

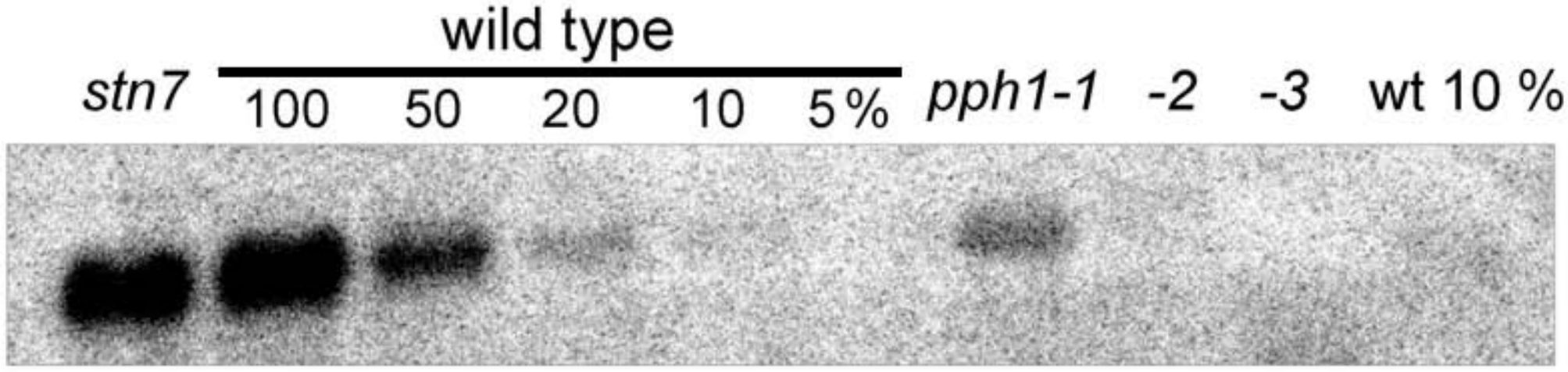
wild type
stn7
100
50
20
10
5 %
pph1-1
-2
-3
wt 10 %
PPH1

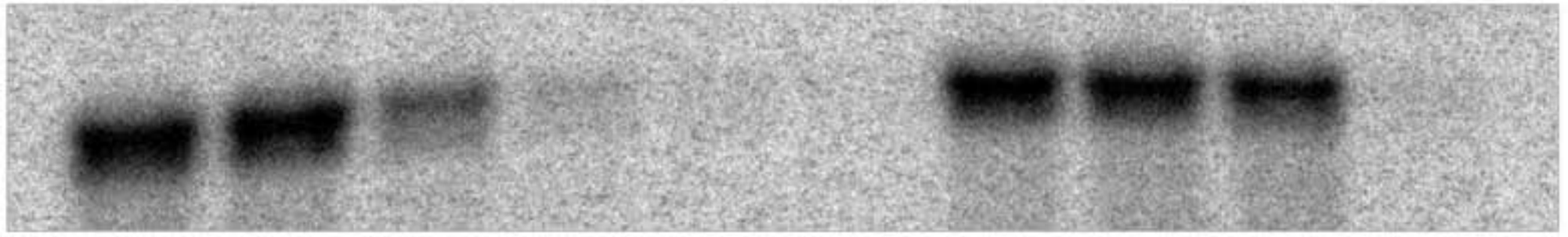
actin

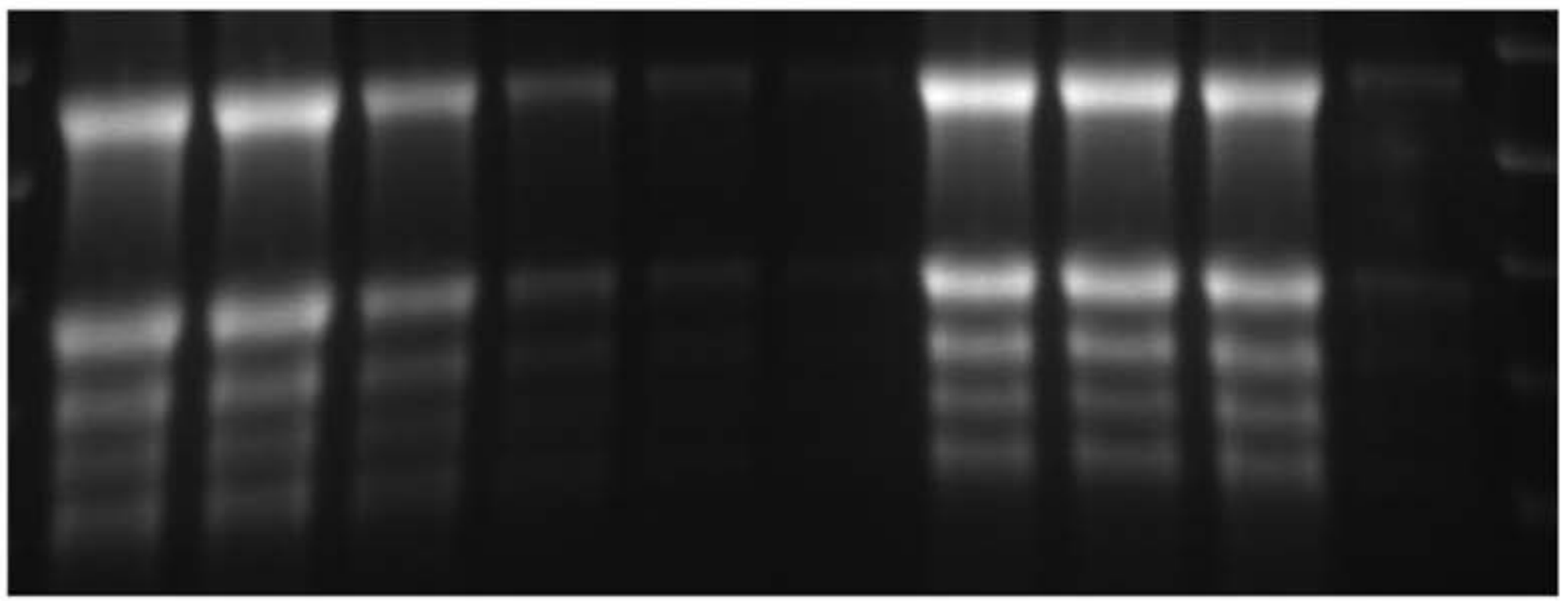
rRNA

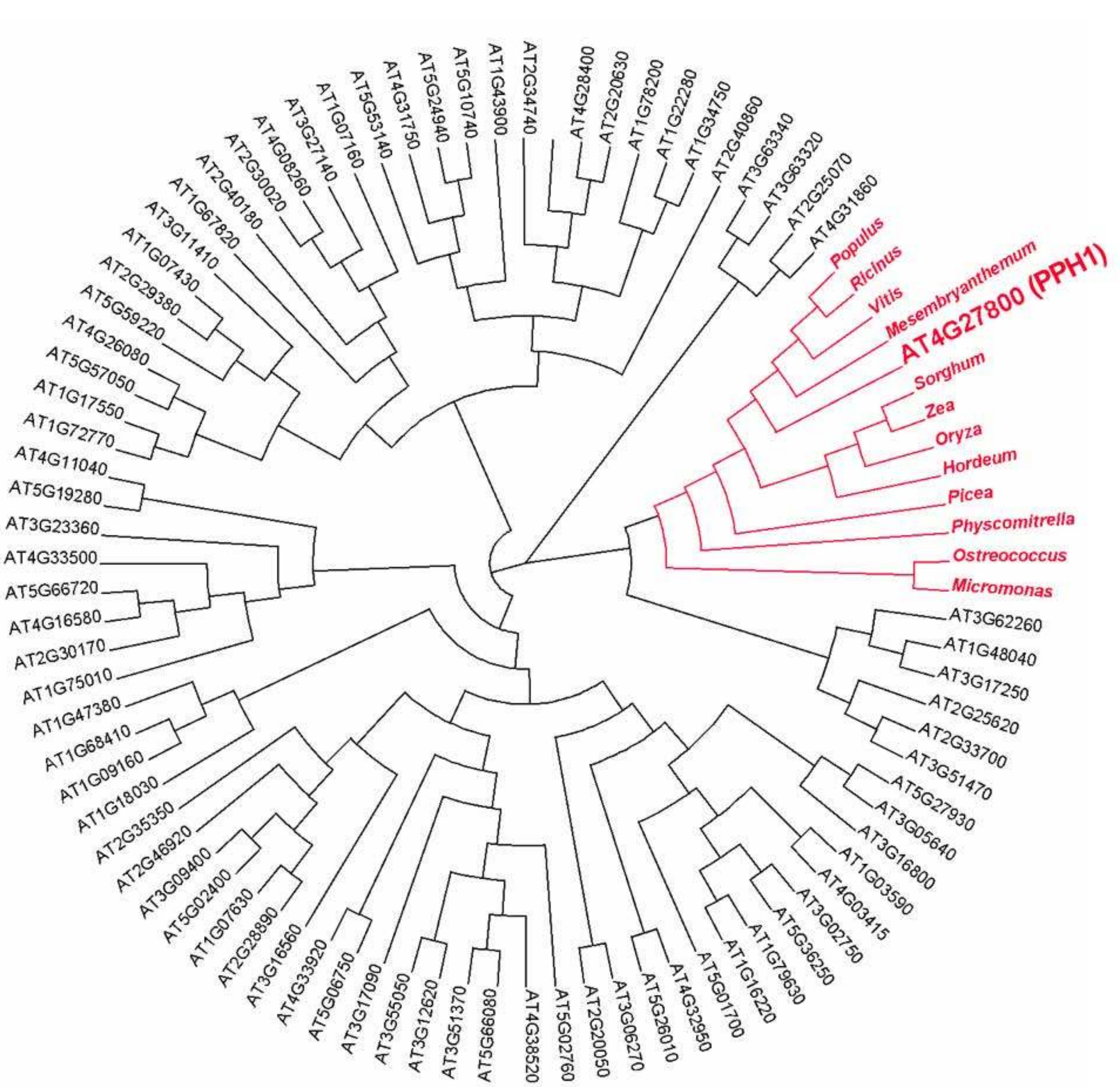
AT4G27800 (PPH1)
Populus
Ricinus
Vitis
Mesembryanthemum
Sorghum
Zea
Oryza
Hordeum
Picea
Physcomitrella
Ostreococcus
Micromonas
AT3G62260
AT1G48040
AT3G17250
AT2G25620
AT2G33700
AT3G51470
AT5G27930
AT3G05640
AT3G16800
AT1G03590
AT4G03415
AT3G02750
AT5G36250
AT1G79630
AT1G16220
AT5G01700
AT4G32950
AT5G26010
AT3G06270
AT2G20050
AT5G02760
AT4G38520
AT5G66080
AT3G51370
AT3G12620
AT3G55050
AT3G17090
AT5G06750
AT4G33920
AT3G16560
AT2G28890
AT1G07630
AT5G02400
AT3G09400
AT2G46920
AT2G35350
AT1G18030
AT1G09160
AT1G68410
AT1G47380
AT1G75010
AT2G30170
AT4G16580
AT5G66720
AT4G33500
AT3G23360
AT5G19280
AT4G11040
AT1G72770
AT1G17550
AT5G57050
AT4G26080
AT5G59220
AT2G29380
AT1G07430
AT3G11410
AT1G67820
AT2G40180
AT2G30020
AT4G08260
AT3G27140
AT1G07160
AT5G53140
AT4G31750
AT5G24940
AT5G10740
AT1G43900
AT2G34740
AT4G28400
AT2G20630
AT1G78200
AT1G22280
AT1G34750
AT2G40860
AT3G63340
AT3G63320
AT2G25070
AT4G31860